Hurricane Andrew's Landfall in South Florida. Part I: Standardizing Measurements for Documentation of Surface Wind Fields

MARK D. POWELL AND SAMUEL H. HOUSTON

Hurricane Research Division, NOAA/AOML, Miami, Florida

TIMOTHY A. REINHOLD

Department of Civil Engineering, Clemson University, Clemson, South Carolina

(Manuscript received 10 April 1995, in final form 8 February 1996)

ABSTRACT

Hurricane Andrew's landfall in south Florida left a swath of destruction, including many failed anemometer recording systems. Extreme destruction led to exaggerated claims of the range of wind speeds that caused such damage. The authors accumulated all available data from surface platforms at heights ranging from 2 to 60 m and reconnaissance aircraft at altitudes near 3 km. Several procedures were used to represent the various types of wind measurements in a common framework for exposure, measurement height, and averaging period. This set of procedures allowed documentation of Andrew's winds in a manner understandable to both meteorologists and wind engineers. The procedures are accurate to ±10% for marine and land observing platforms, and boundary layer model adjustments of flight-level winds to the surface compare to within 20% of the nearest surface measurements. Failure to implement the adjustment procedures may lead to errors of 15%–40%. Quality control of the data is discussed, including treatment of peak wind observations and determination of the radius of maximum winds at the surface.

1. Introduction

Hurricane Andrew's landfall in south Florida on 24 August 1992 (Mayfield et al. 1994) ranks as the worst natural disaster in U.S. history in terms of destruction and property loss. Andrew was the first Saffir–Simpson (Simpson and Riehl 1980) category 4 hurricane to strike a major urban area in Florida since Donna in 1960. Hurricanes of similar intensity to Andrew may become more frequent in the Atlantic basin if climatic influences on circulation patterns lead to a return to a period of active hurricane formation and landfall (Landsea 1993).

Immediately following Andrew, great interest arose regarding the magnitude and extent of the winds responsible for both the widespread damage and the localized swaths of destruction. Unsubstantiated rumors circulated in the media of extreme sustained winds ''clocked'' anywhere from 150 to 214 mph at several locations (the Pioneer Museum, Turkey Point nuclear power plant, Homestead Air Force Base, and a U.S. Army communications facility) where wind records were nonexistent or incomplete. These rumors took on a life of their own and still persist with the public; many residents feel that they have survived a storm with winds much worse than actually occurred.

A controversy developed after a preliminary report from the Wind Engineering Research Council (WERC 1992) suggested weaker winds than those issued in advisories and a preliminary report by the National Hurricane Center (NHC 1992). Additional reports based on damage investigations and model simulations fueled the controversy (Wallace 1992). The implications of these and other wind studies would influence the outcome of millions of dollars worth of litigation related to storm damage. Two sides of the wind speed issue emerged: 1) Andrew was an act of God and it is impossible to economically design and build a structure to withstand such winds, and 2) Andrew's winds were no stronger than other recent hurricanes such as Hugo in 1989; with good workmanship and proper safety factors taken into account, structures should have been able to hold up to the wind loading. The merits of these viewpoints are still being argued in the courts. Compounding the controversy was the tendency for meteorologists and wind engineers to use different terminology and procedures for dealing with surface wind measurements and analyses.

The purpose of this paper is to outline a series of analysis methods for hurricane wind observations that produce wind fields in a common framework for both

Corresponding author address: Dr. Mark D. Powell, Hurricane Research Division, NOAA/AOML, 4301 Rickenbacker Causeway, Miami, FL 33149.
E-mail: powell@aoml.noaa.gov

© 1996 American Meteorological Society

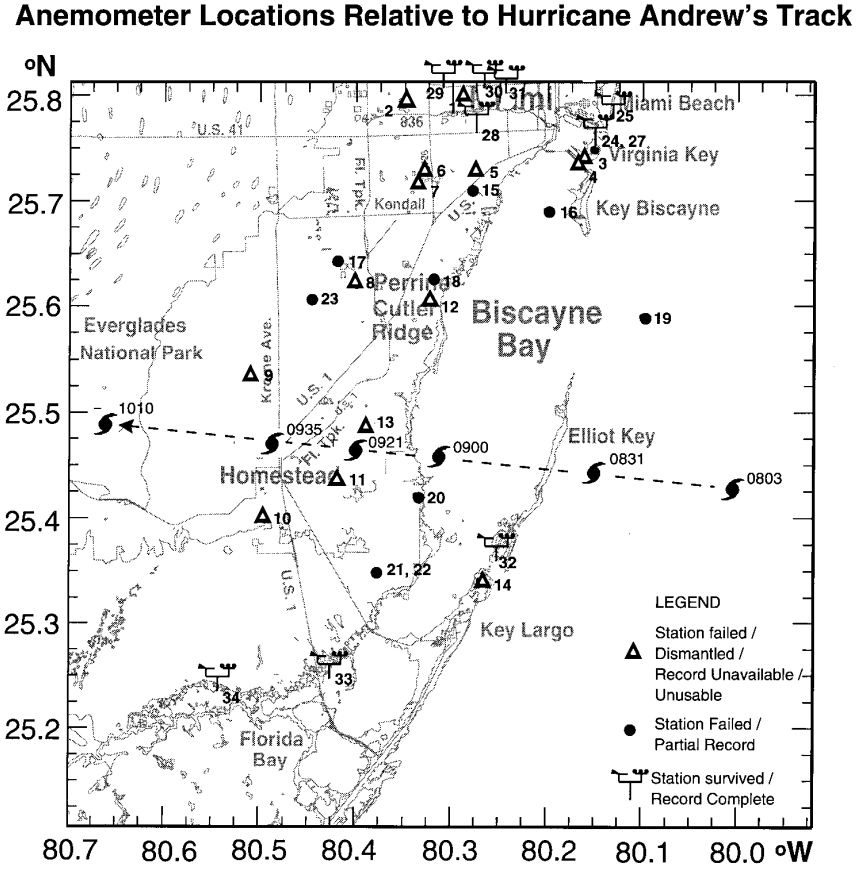

FIG. 1. Track of Hurricane Andrew's wind center, with locations of surface observations and their survivability. Numbers refer to sources listed in Table 1. Site 26 (not shown) is about 12 km north of site 25.

meteorologists and wind engineers. These methods conform to accepted practice in the fields of micrometeorology and wind engineering and design and are being employed in a surface wind analysis system under development for eventual transfer to NHC.

This paper will first discuss failures of anemometer systems relative to Andrew's track and strategies for improving their performance. The turbulent and convective characteristics of hurricane winds will then be considered as suggested by spectral density calculations from several storms. The importance of a common observing framework will be highlighted, stressing height adjustment to the reference level of 10 m and its dependence on roughness and stability over land and offshore. Adjustment to standard terrain (open exposure) over land follows, together with the determination of the maximum 1-min sustained wind speed based on gust factor data and averaging period. Finally, quality control of the Andrew dataset is described, including consideration of the placement of adjusted reconnaissance wind observations. The companion paper (Powell and Houston 1996) describes objective analyses of Andrew's strongest surface winds, wind field decay over south Florida, and potential applications for real-time analysis and preliminary damage assessment.

2. Data availability and anemometer system problems

The storm track (Fig. 1) represents the track of the circulation center, based on wind measurements from U.S. Air Force Reserves reconnaissance aircraft at 3-km altitude and public reports of calm observed at the surface; positions of wind measurement sites are also plotted. Wind measurement systems failed for a variety of reasons (Table 1) including lack of recording capability and mast, crossarm, and guy wire failures caused by a combination of design faults, high winds, and debris. Most sites were installed for a specific purpose: aviation, air quality, agriculture, general interest. In our opinion, very few sites would have failed if they were installed to survive hurricane episodes. The fact that several instruments survived that lacked

TABLE 1. Anemometer survival in Hurricane Andrew: complete, partial, and failed sources.

Size	Comments
Station failed or dismantled, record unavailable or unusable (14)	
1. NOAA/NWS/MIA	Electrical problem station out before storm
2. FAA/LLWAS	One station performed erratically
3. NOAA/AOML	Dismantled to protect atrium windows
4. UM/RSMAS	Dismantled to protect sensors used for climate program
5. UM/engineering	Inadequate information on sampling
6. Metro Dade/emergency operations center	No recording capability, log unavailable
7. Metro fire/rescue	No recording capability, log unavailable
8. Army communication site	No recording capability, no log
9–11. Agricultural extension service	Three sites had central datalogger waterlogged and shorted
12. Metro Water and Sewer pump 5	Mast failed, chart record timing error, calibration error
13. Homestead AFB	Power turned off to wind recorder before storm
14. Ocean Reef emergency operations center	Station dismantled for maintenance
Station failed with partial record (10)	
15. NOAA/NHC (NHC)	Crossarm rotated, dropped sensor to roof
16. Seaward explorer	No recording capability, manual obs
17. FAA/Tamiami Airport	No recording, manual obs, crossarm rotated, mast failed
18. Perrine homeowner (PER)	No recording capability, manual obs, mast failed
19. Fowey Rocks C-MAN	Mast failed at base attachment after 0800 UTC
20. FPL 1 Turkey Point	Mast failed, cups blown out of frames
21, 22. FPL 2 60-m mast (two sensors)	Cups blew out of frames, no backup power
23. Agricultural Extension Service	No obs transmitted after 0730 UTC (one ob only at Glider Port)
24. Metro Water and Sewer at Virginia Key 1	
Station survived with complete record (10)	
25. NOAA/Miami Beach DARDC	
26. NOAA/NOS Next-Generation Water Level site at Haulover Pier	
27. Metro Water and Sewer at Virginia Key 2	
28–31. FAA/LLWAS (four sites) at Miami International Airport	
32. Sailing yacht *Mara Cu*, North Key Largo	
33. National Park Service station at Manatee Bay	
34. National Park Service station at Joe Bay	

recording capability is disturbing. ''Eyewitness'' observations from the digital or analog display of sites without recorders were extremely difficult to document and confirm. In particular, determining the time and duration of extreme winds observed in this manner was especially difficult.

An example of one type of failure suffered by anemometers installed by the Federal Aviation Administration (FAA) and by the National Weather Service (NWS) is shown in Fig. 2. This type of failure occurred at Tamiami Airport and at NHC. Conduit pipe used for the crossarm unscrewed itself when subjected to torque produced by the drag force on the anemometer. Once rotated past 90 degrees, the relatively heavy weight of the instrument contributed to pull the instrument out of its mounting socket and onto the ground. Afterward, the mast was hit by debris visible in Fig. 2. The added drag on the mast pulled one of the guy wires out of the ground, causing the mast to topple. Unfortunately, this site had no recording capability. The mast at NHC did not topple, but the anemometer fell off the crossarm in an identical manner. After a recommendation by the Interdepartmental Hurricane Conference (OFCM 1993a), a retrofitting kit was developed to lock the crossarm on similar systems. In addition, the Automated Surface Observing System (ASOS) anemometer design is also being studied for similar failure potential.

The highest surface winds measured in the storm came from anemometers (Perrine and Fowey Rocks C-MAN) that experienced mast failures shortly afterward. As discussed below, both measurements occurred in the northern eyewall, in close proximity to the maximum 10-s flight-level winds measured by the air force reconnaissance aircraft. Although it is possible that slightly higher winds occurred after the failures, we believe that these measurements adequately sampled Andrew's maximum sustained winds and that subsequent winds were not significantly higher.

The problems with wind data availability summarized in Table 1 are not unique to Andrew; these difficulties plague all major tropical cyclone landfalls worldwide. The most promising strategies for improving the availability of hurricane wind measurements

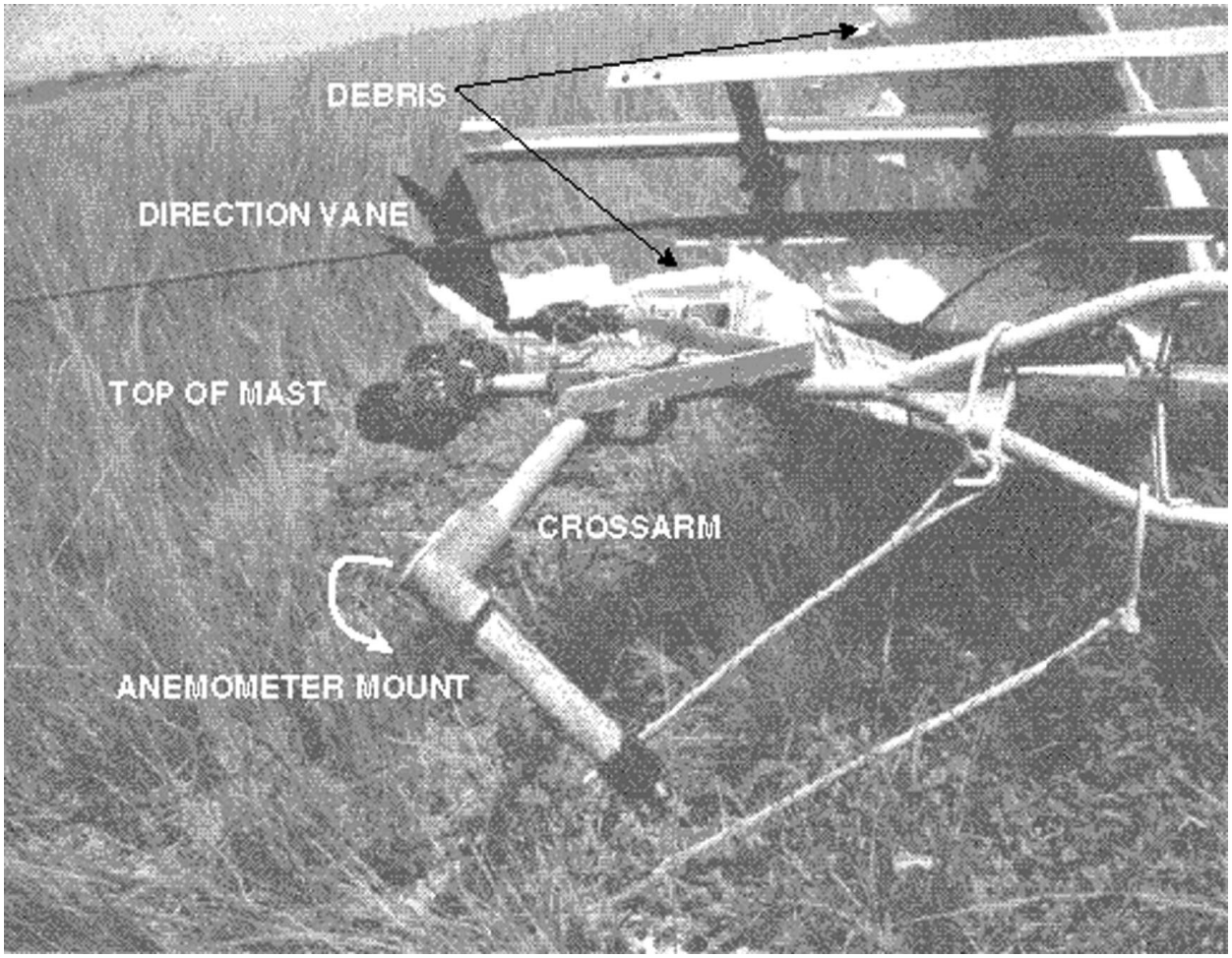

FIG. 2. F-420 anemometer failure at Tamiami Airport. Note rotation of crossarm (shown by arrow), which allowed anemometer to be twisted off its mounting.

include the following: 1) Incorporate recording capability on all current anemometer systems and inspect instrument masts for survivability. 2) Adopt a surface wind measurement standard containing guidelines for survivable anemometer performance characteristics, siting, emergency power, and archival recording that is consistent with recommendations of the World Meteorological Organization (WMO). A draft standard has been submitted to the American Society for Testing of Materials for consideration as a standard (T. Lockhart, Meteorological Standards Institute, 1994, personal communication), based in part on reaction to limitations of the ASOS system (Powell 1993). 3) Support of a university/federal agency/private industry network of preidentified anemometer sites that can either be instrumented each hurricane season or rapidly deployed locally when a hurricane is approaching. This deployment approach has the advantage of local logistics to allow enough time for proper installation of a measurement site.

3. Hurricane wind characteristics

a. Spectral density

If meteorologists and wind engineers hope to adequately measure the wind field of landfalling tropical cyclones, it is imperative that we learn as much as possible about processes that influence the flow field and its temporal and spatial scales. Typically, the only information available to study such processes has been strip chart records from landfalling hurricanes and typhoons, and these records suffer from poorly documented response characteristics of the chart–sensor system. A few digital time series were collected by Brookhaven National Laboratory (BNL) on Long Island, New York, for several landfalling hurricanes in the 1950s and 1960s, by the Ocean Current Measurement Program for two hurricanes in the Gulf of Mexico, and by the Field Research Facility of the U.S. Army Corps of Engineers (USACE) Coastal Engineering Research Center at Duck, North Carolina, for

Hurricane Bob in 1991. Unfortunately, no high-resolution time series data of this type were recorded in Hurricane Andrew, but the spectral density characteristics from these other datasets may shed some light on the scales of motion that may have been present.

BNL tower observations were collected in Hurricanes Carol (1954), Edna (1954), Connie (1955), and Donna (1960) at ~100 m as described in van der Hoven (1957), Davenport (1961), and Singer et al. (1961). Mean wind observations in these storms ranged from 20 to 29 m s^{-1}. Van der Hoven (1957) used the Connie observations together with longer, nonhurricane time series records to establish the existence of a mesoscale spectral gap at periods corresponding to 0.1–5.0 h. Davenport (1961) examined several high-wind datasets, including Hurricanes Carol and Edna. His spectral density plots were normalized by the estimated surface stress. All the BNL spectra show a hump shape beginning with a magnitude of 0.5 m^2 s^{-2} at a frequency of 2 h^{-1}, reaching a peaks of 3–20 m^2 s^{-2} at 50 h^{-1} (1.2 min) and then trailing off at higher frequencies of 10^3 h^{-1}. BNL is situated in an open field amid a scrub pine forest, resulting in a roughness length of 1 m. Forristall (1988) analyzed wind spectra collected from offshore oil rig platforms in the Gulf of Mexico during Hurricanes Eloise (1975) and Frederic (1979) in mean winds of 29 m s^{-1} at the 40-m (Eloise) and 70-m (Frederic) levels. His spectral density plots were normalized by the wind variance and showed a similar shape to those from BNL over a frequency band from 0.3 to 3600 h^{-1} with a peak of 20%–30% of the variance (or ~3 m^2 s^{-2}) at 30–300 h^{-1} (0.2–2.0 min).

Spectral density analysis of Hurricane Bob (Fig. 3) in a mean alongshore flow of ~23 m s^{-1} (at 20-m level) show agreement with previous studies in the shape of the spectrum but display much lower peak energy levels (0.2–0.3 m^2 s^{-2}) at 20–300 h^{-1} (0.2–3.0 min) in accordance with lower wind speeds and smoother terrain. All the spectra are dominated by turbulent (100–2000 h^{-1}, 2–30 s) and convective mesogamma (10–100 h^{-1}, 0.5–6.0 min) scales, with no evidence of larger mesoscale phenomena. In lower speeds, however, the Hurricane Bob data (not shown) show evidence of considerable energy in mesogamma and mesobeta scales (0.5–10 h^{-1}, 6–30 min) that may be associated with rainbands or boundary layer roll vortices (Tuttle and Gall 1995). The effects of rainbands and individual convective elements on spectral shape would probably also be dependent on the track of the storm relative to the measurement site. In Andrew, with surface winds of 40–60 m s^{-1}, it is likely that the peak in the spectrum would be found at the turbulent and convective-mesogamma scales. Applying Davenport's (1961) normalized spectrum shape to Andrew would yield peak energy for open terrain on the order of 10–20 m^2 s^2.

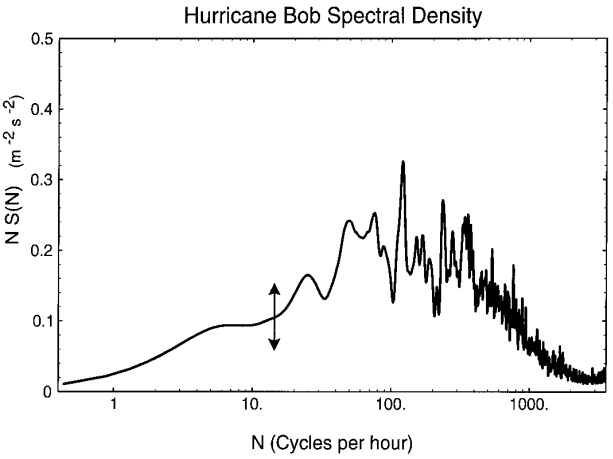

FIG. 3. Spectral density plot of detrended fluctuations of the streamwise component of the wind at 20 m measured at the USACE Duck, North Carolina, pier for alongshore flow in 23 m s^{-1} mean winds during Hurricane Bob on 19 August 1991. Spectral estimates have been smoothed with a 20-point Hanning filter. Vertical axis is the product of frequency and spectral density, which has units of variance; horizontal axis is frequency expressed in cycles per hour on a logarithmic scale. The vertical line with arrows refers to the 95% confidence interval applied to an estimate of 0.1 m^2 s^{-2}. The area beneath the curve is proportional to the contribution of a given frequency band to the total variance.

b. Applicability of similarity theory

A method is required to adjust winds to a common height, exposure, and averaging time. Height and exposure adjustment procedures depend on relationships developed from Monin–Obukov similarity theory. According to Panofsky and Dutton (1984) and Arya (1988), similarity requires a horizontally homogeneous surface layer where the mean flow and turbulent characteristics depend only on height, surface stress, surface heat flux, and buoyancy. The flow is assumed to be quasi-stationary, turbulent fluxes of momentum and heat are assumed independent of height in the surface layer, and molecular and rotational effects are negligible. Hence, the wind direction is constant within the surface layer, and the variation of wind speed with height is controlled by the surface stress, terrain roughness, and surface heat flux. To the extent that turbulent and smaller convective scales are important, the characteristics of the flow should be well represented by surface-layer similarity theory. If the fluctuations of the flow are primarily affected by cloud- and rainband-scale phenomena, surface-layer similarity may fail to consider important scaling parameters. In a hurricane, rotational effects associated with curved flow may also be important. The motion of a storm makes it unlikely that quasi-stationarity can be satisfied except for short time periods in slow-moving storms. Even though the mean flow may be changing with time, the distribution of short-period means about longer-period means may not change greatly from one time period to the next.

For example, histograms of deviations of the 1-min mean wind about the 10-min (Fig. 4a) and 1-h means (Fig. 4b) from data collected in Hurricane Bob suggest a Gaussian distribution. Closer to the eyewall, or for a faster-moving storm like Andrew, considerable changes can occur over 1 h, but periods of order 10 min would be relatively stable.

Despite these inadequacies, similarity-based procedures and boundary layer adjustment models appear to work reasonably well and have been used to adjust flight-level reconnaissance measurements to the surface (Powell 1980) and also to reconstruct hurricane wind fields at landfall (Powell 1982, 1987; Powell et al. 1991). In this paper, subject to the limitations discussed above, we will assume that 1) similarity theory relationships are applicable for height adjustment of measured winds and 2) gust factor relationships developed under the Gaussian assumption are applicable for estimating short period wind extremes from longer period averages, or vice versa.

4. Standardization of Hurricane Andrew wind measurements

To analyze the surface wind field accurately, it is critical that input data conform to a common height, averaging period, and exposure. Wind observations uncorrected for height, fetch, and time period may show large differences over short distances (caused by terrain roughness and associated turbulence) that mask larger-scale wind features associated with the storm. Objective analysis filters can smooth out these differences, but unrepresentative information will then become part of the analyzed field. Our approach to the reconstruction of Andrew's wind field is to standardize input observations to a common reference framework before analysis. The standardization generally requires a five-step process (Fig. 5): 1) compute the mean (10 min) surface wind from continuous short-period means (if available) or extreme short-period means (by use of gust factor relationships), 2) determine the observation exposure type, 3) adjust to the reference height (10 m), 4) adjust to the reference exposure, and 5) adjust to the maximum sustained (1-min mean) wind over the averaging period. Step 1 is required because the surface-layer similarity relationships used in steps 2–4 require a mean wind and the 10-min mean is a more stable measurement of the mean wind than a 1-min mean. These steps also apply to determination of peak winds for engineering applications, except that step 5 refers to a peak 3-s wind speed (ASCE 1994). Each step is documented below along with estimates of the uncertainty and consequence error.

As an example, consider the FAA Low Level Windshear Alert System (LLWAS) measurements collected in the vicinity of Miami International Airport, about 36 km north of Andrew's wind center. This location was not affected by Andrew's eyewall, but LLWAS recorded a dense collection of wind measurements from which spatial variability of the wind field could be studied. One-minute averages computed from these data for 0935 UTC 24 August are displayed in Fig. 6a, along with anemometer heights Z_{AN}, estimated roughness lengths Z_O, and zero-plane displacement heights Z_D (described below) based on site visits and photographic descriptions of the site exposures. The variance of the wind observations displayed in Fig. 6a is considerable (19.6 $m^2\ s^{-2}$) with the wind speeds varying by more than a factor of 2 between the lowest and highest observations. These differences are due to many factors, including anemometer height, exposure differences, and the natural variability of the wind associated with turbulent eddies and convective cells over a 50 km^2 area. After averaging the data for a longer period (10 min), adjusting the observations to a common height of 10 m, and further adjusting the observations to a common exposure typical of an airport runway (Fig. 6b), the variance is reduced to 3.6 $m^2\ s^{-2}$, a reduction of 79%.

A closer look at the exposures of these sites helps to account for the differences; site FA1 (Fig. 7a) was the open exposure site in the middle of the runway grid, sites FA2 and FA4 were in suburban terrain north and south of the airport, and site FA3 (Fig. 7b) was exposed very poorly to the east of the airport. Without information on the instrument exposure and height, one might expect the sites to be comparable and conclude that the observed differences in wind speed were caused by some small-scale feature associated with the storm. As weather services are modernized, it is hoped that all wind sites will eventually be catalogued for exposure and sensor height, allowing standardization of measurements to an exposure representative of a desired analysis product or consistent with numerical weather prediction model land use and roughness specifications.

a. Determination of exposure

In most cases the upwind fetch of a wind observation can be roughly categorized as either ''land'' or ''marine.'' For coastal stations, stations just inland or just offshore, the fetch depends upon whether the wind direction is on-, off-, or alongshore. Winds proceeding from sea to land decelerate and form an internal boundary layer (IBL, Fig. 8); winds from land to sea accelerate. For neutral and for unstable conditions, the height of the IBL may be approximated (Peterson 1969; Wood 1982; Arya 1988) by

$$h_I = cZ_{OR}\left(\frac{X}{Z_{OR}}\right)^{0.8}, \qquad (1)$$

where c is a constant dependent on stability with values between 0.28 and 0.75, Z_{OR} is the larger of the two roughness lengths, and X is the distance downwind of

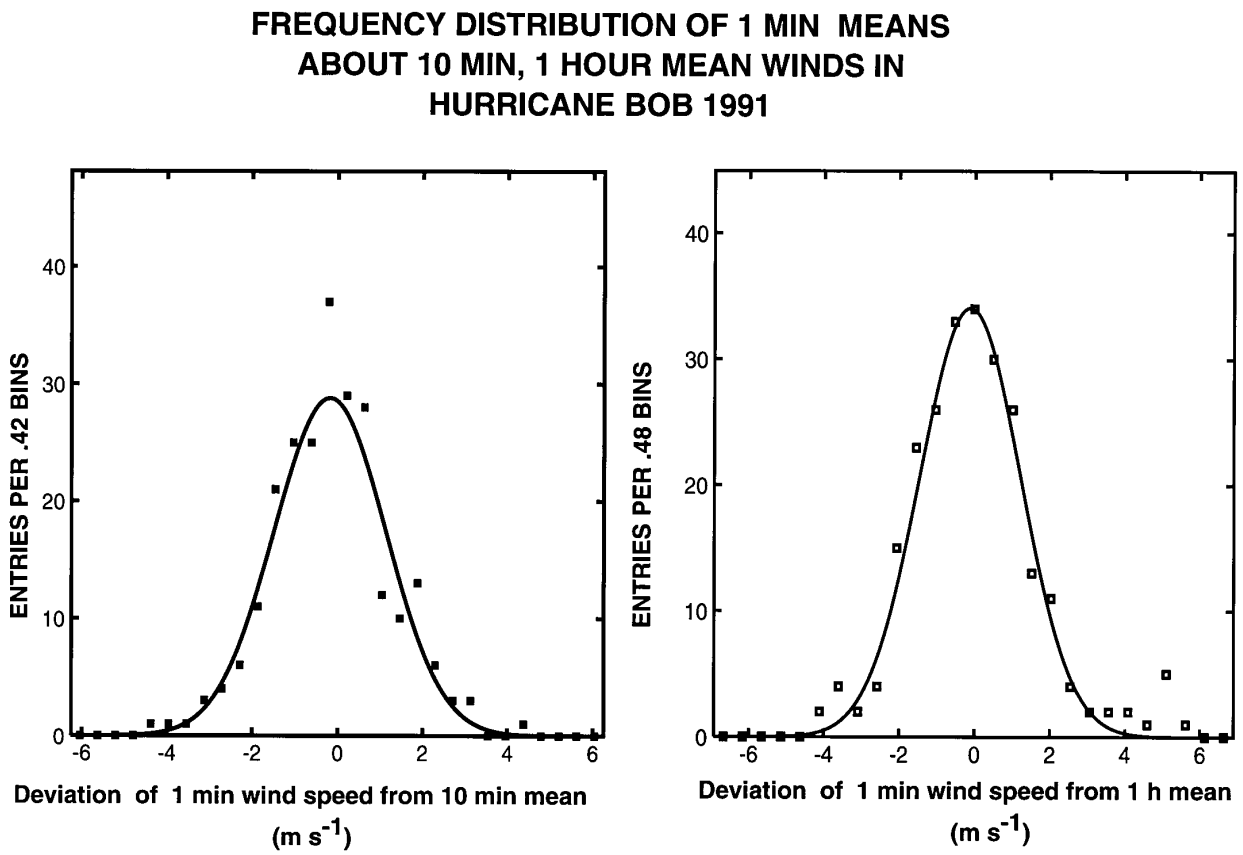

FIG. 4. Histogram of the deviations of 1-min means about (a) 10-min means and (b) 1-h means observed during Hurricane Bob at the USACE Duck, North Carolina, pier on 19 August 1991. Curves represent fits of a Gaussian distribution to the data. The vertical axis refers to the number of observations within a 0.42 m s^{-1} (left) or 0.48 m s^{-1} (right) bin.

the roughness change. Winds above h_I are the same as would be measured over the upwind roughness. Winds below $h_E = 0.1h_I$ are in equilibrium with the new roughness, and between h_E and h_I, the wind is in the process of adjusting to the new underlying roughness. By estimating Z_{OR} as described below, measuring X from a map or navigation chart, and comparing h_E to the Z_{AN} of the station of interest, one can estimate the exposure category according to whether Z_{AN} is closer to h_I (same category as the upwind roughness) or h_E (same category as the downwind roughness).

Onshore airflow can experience several additional IBL formations depending on land use and topography. In such conditions, a wind profile with sufficiently long averaging times might show kinks associated with separate h_I values or a new transitional boundary layer may be evident that has not reached equilibrium with the new underlying surface. Furthermore, in the early hours of an approaching hurricane or the late hours following landfall, the wind direction may parallel the coastline. In this situation it is difficult to characterize the exposure because transverse eddies in the upstream flow field will cause the wind to have characteristics of either land or marine or a combined exposure.

The failure of the flow to reach equilibrium was readily apparent when comparing observations from the LLWAS system. The extreme north and south stations, FA2 and FA4, were both in suburban terrain with roughness lengths estimated at 0.5–1.0 m based on the guidelines of Wieringa (1992). These estimates performed well in adjusting anemometer heights to 10 m and open-terrain exposure (as defined by comparison to FA1 observations) when wind directions were from the north (overland fetch). However, when the wind veered to the northeast, open-terrain-adjusted winds at FA2 and FA4 (using the assigned roughness lengths) failed to compare with FA1. Apparently, the distant marine fetch (even at 20–30 km upwind) became important, and roughness estimates had to be reduced (Fig. 6) to produce good comparisons to FA1. This behavior of higher-estimated versus lower-measured (from wind profile) roughness was observed for flow from sea to land for fetches up to 45 km inland in Denmark by Sempreviva et al. (1990). Models attempting to deal with multiple IBL formation along a downwind trajectory have been developed by Larsen et al. (1982). Conceivably, such models could predict downwind flow based on a knowledge of roughness lengths along

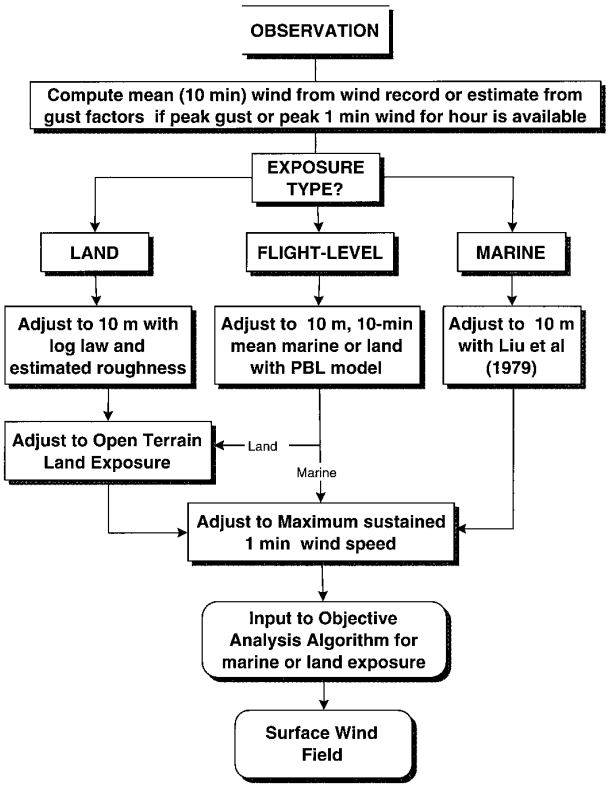

FIG. 5. Flow chart of procedures necessary to achieve a common framework for analysis of hurricane wind observations.

the trajectory. In a hurricane the flow trajectory is complicated by additional accelerations associated with the pressure field, the radial distance from the storm center, and convective components associated with updrafts and downdrafts in the eyewall and rainbands.

b. Adjustment of wind measurements to 10 m

Surface winds in hurricanes can vary greatly horizontally depending on the roughness of the upwind terrain and the distribution and size of obstacles along the flow. This variability was readily apparent in ground and aerial observations of the damage field after Andrew. Structures exposed to flow over open terrain were much more susceptible to damage than those sheltered by surrounding houses or trees upwind. Although most NWS and FAA weather stations and forecast offices prescribe open exposures for installation of wind measuring equipment, not all anemometers are in compliance, and much variability exists in the private sector. For meteorological applications the height recommended by the WMO for wind measurement is 10 m above ground level. To properly adjust winds to a common height, the upwind fetch roughness must be known. Similarity relationships form the basis for height correction of wind speed measurements discussed below; wind directions are assumed to be independent of height in the surface layer.

1) LAND EXPOSURE

Mean surface wind measurements U_z at a height $Z > Z_D$ m above the surface are adjusted to the 10-m-level wind speed U_{10} (assuming neutral stability conditions) according to

$$\frac{U_{10}}{U_z} = \frac{\ln[(10. - Z_D)/Z_O]}{\ln[(Z - Z_D)/Z_O]}. \qquad (2)$$

Values for Z_O were based on categories published in Panofsky and Dutton (1984), Wieringa (1992), and Simiu and Scanlan (1986). When exposure is influenced by a uniform distribution of objects (e.g., houses, trees) that are large relative to the height of the anemometer, the zero-plane displacement height (Z_D) is used to estimate the effective height ($Z - Z_D$) of the anemometer above the surrounding roughness elements [Z_D is approximately 75% of the mean height of the objects (Arya 1988)]. It should be kept in mind that roughness estimation is very much an art; reasonable estimates of roughness by experienced investigators can vary by as much as 0.25–0.50 m. For a mean wind speed of 35 m s^{-1} at 20 m in neutral atmospheric stability with $Z_D = 0.0$, this difference in estimates of Z_O would correspond to 10-m-level winds of 29.5 m s^{-1} ($Z_O = 0.25$ m) and 28.4 m s^{-1} ($Z_O = 0.50$ m), respectively. Similarly, an adjustment of a 35 m s^{-1} wind from 5 m would result in 10-m-level winds of 43.1 and 45.5 m s^{-1}, respectively. These calculations imply a velocity uncertainty of $\pm 7\%$ for a 0.25-m difference in roughness length estimation. In contrast, based on these examples, failure to adjust winds to a common reference height could lead to errors in wind estimates at a given level of 15%–30%. This error becomes much larger as the difference between actual anemometer height and the standard reference height increases.

2) MARINE EXPOSURE

Despite recent studies of drag, heat, and moisture coefficient dependence on wind speed, most notably the Humidity Exchange Over the Sea experiment (Katsaros et al. 1987), few observations are available to test the suitability of these relationships in hurricane force wind speeds. We use the same model (Liu et al. 1979) employed operationally by the National Oceanic and Atmospheric Administration (NOAA) National Data Buoy Center for the reduction of Coastal Marine Automated Network (C-MAN) and buoy mean winds to the 10-m level. The model is also used to calculate the roughness length for determining surface stress from lowest-level eta model winds over the ocean (Janjic 1994). This model includes interfacial sublayers close to the sea surface where molecular effects on transports are important. Surface stress and roughness

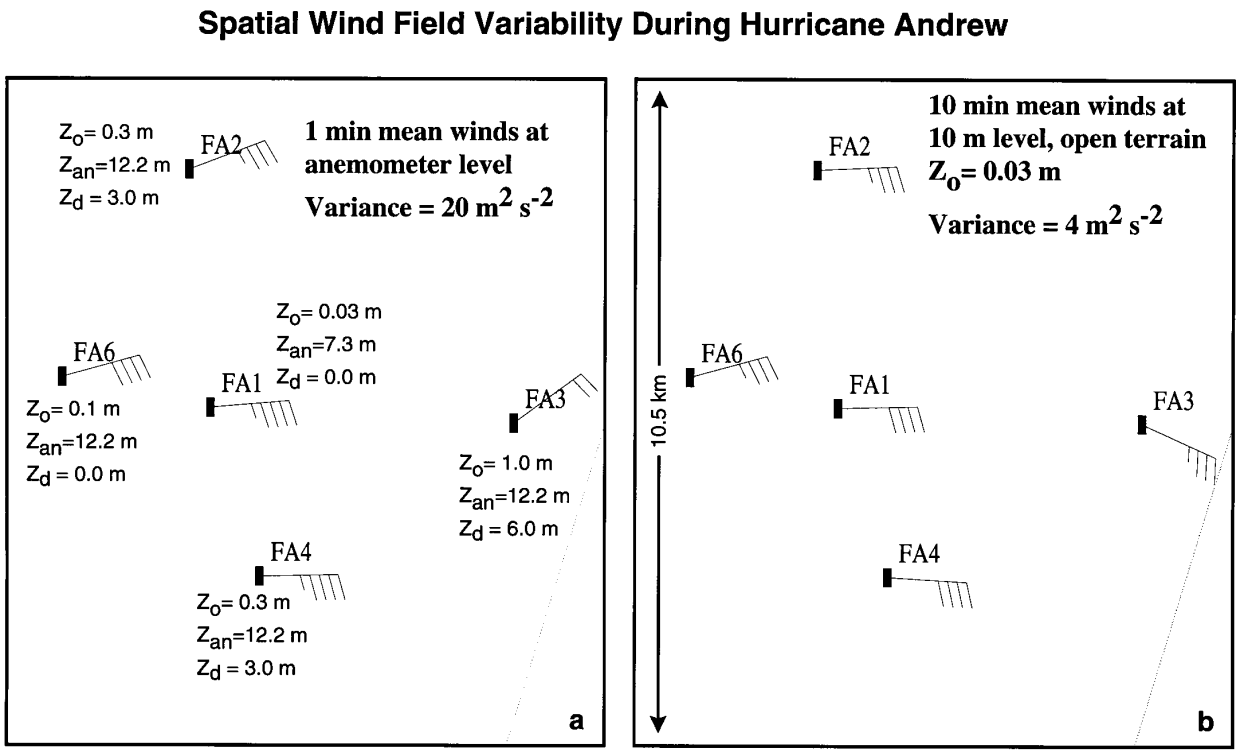

FIG. 6. LLWAS data in the vicinity of Miami International Airport for 0934 UTC during Hurricane Andrews landfall. (a) Roughness lengths (Z_O), anemometer heights (Z_{AN}), zero-plane displacement heights (Z_D), and wind barb plots of the 1-min mean wind observations at 0934 UTC. (b) 10-min mean wind observations centered on 0934, adjusted to 10 m and open terrain. Wind barb convention is 25 m s^{-1} for a triangle, 5 m s^{-1} for a single barb, and 2.5 m s^{-1} for a half barb.

are computed according to stability as determined by the air–sea temperature difference. For hurricane winds, the model was configured to use the drag coefficient dependence on wind speed developed by Large and Pond (1981).

As discussed by Liu et al. (1979), this model's treatment of interfacial sublayers may be suspect at high wind speeds, especially when spray effects alter temperature and humidity profiles in the surface layer. The effect of ocean wave age on sea surface stress (Janssen 1989) may also be important; in a fast-moving hurricane like Andrew, where the wave field at any point is subject to changing wind speed and directions, the sea surface may be rougher than a fully developed sea. Hence, the changing wave field could act to further increase uncertainty in the roughness.

For 10-min mean winds of 30 and 60 m s^{-1} at Z_A = 39 m at Fowey Rocks C-MAN station, the Liu et al. (1979) model computed Z_O at 0.007 and 0.015 m, respectively. The Z_O value of 0.015 m is close in magnitude to values of Z_O = 0.03 m normally attributed to open-terrain land roughness. Based on these roughness calculations, for winds on the order of 60 m s^{-1}, one should expect little change in mean wind speeds when flow progresses from the ocean to land with open-terrain characteristics. Because of characteristically smoother roughness values over water relative to those over land, errors in roughness length parameterization are smaller than those estimated over land. For a ±0.002-m variation in roughness length about a value of 0.01 m, the wind speed difference is about ±3%. Failure to adjust marine wind speeds to 10 m will result in errors comparable to those previously mentioned for land exposures (i.e., 15%–30%).

3) ADJUSTMENT OF FLIGHT-LEVEL WINDS

During Andrew's landfall, air force reconnaissance aircraft recorded data at a flight-level of 2.5–3.2 km and transmitted the observations in real time to NHC via an aircraft–satellite data link. For the flights on Florida's southeast coast, the wind data consist of consecutive 1-min means and the peak 10-s mean within each minute; complete 10-s data were not available. For the flights on Florida's southwest coast, complete consecutive 10-s and 1-min mean wind data were available. The data were collected along radial flight tracks extending from the eye to over 220 km outward. Positions and wind measurements are determined via the Self-Contained Navigation System (SCNS), based on solutions determined from an inertial navigation unit. Position accuracy is advertised as ±4.3 km; actual ac-

FIG. 7. Examples of contrasting exposures for LLWAS sites FA1 (a) and FA3 (b) plotted in Fig. 6.

curacy is probably much better since typical terminal errors are less than ±2 km (R. Katz, SCNS program manager, 1993, personal communication). Reconnaissance aircraft attempt to meet or exceed accuracy requirements of ±2 m s^{-1} for flight-level wind speed and ±5° for wind direction (OFCM 1993b). No intercomparison flight data were available for Andrew or any other hurricanes during the 1992 season. An intercomparison of NOAA and air force aircraft conducted in Hurricane Emily of 1993 and analyzed by the authors discovered occasional dropouts or negative spikes in the air force 10-s mean data on outbound southward and inbound westward flight legs (see Black and Houston 1994 for more details). These problems were caused by errors in the aircraft data processing software that have since been corrected. Accordingly, for the southeast coast landfall analysis, one outbound southward flight leg was removed (two northward inbound legs covered the same area) and only peak 10-s flight-level data were considered for the inbound westward flight leg (where no additional flight legs were available near the time of landfall). For the flight covering Andrew's emergence over the Gulf of Mexico, complete 10-s data were available. Time series of these data were examined for obvious spikes and dropouts, which were edited from the dataset.

Flight-level observations are adjusted to the surface with a planetary boundary layer (PBL) model (Powell 1980). Flight-level winds are assumed to be representative of mean winds in the boundary layer and Deardorff's (1972) deficit law approach is followed to adjust this wind to the top of the surface layer. The model iterates on a friction velocity solution, and then a 10-m-level wind is computed according to similarity theory using a roughness of 0.03 m over land and a roughness over water based on the Charnock (1955) relationship with constant $\alpha = 0.0144$ (Garratt 1977). The 10-m wind computed by the model is assumed to be equivalent to a 10-min mean measured by a marine surface station; this quantity is then adjusted (see below) to a maximum 1-min mean that would be expected within a 10-min period. Thermodynamic input

to the model assumed neutral conditions over land in the vicinity of the eyewall (surface temperature 0.1°C cooler than the air temperature), slightly stable conditions (surface temperature 1.0°C less than air temperature) radially outward from the core over land (radii greater than 34 km), and unstable conditions throughout over water (sea surface temperature 3.5°C warmer than the air) as observed by Fowey Rocks C-MAN station. Adjustment ratios from this model were inversely proportional to the magnitude of the bulk Richardson number [defined as $gZ_B\Delta T_{A\text{-}S}/(T_A V^2)$], where g is gravitational acceleration, Z_B is the boundary layer height (assumed 750 m), $\Delta T_{A\text{-}S}$ is the air–sea virtual potential temperature difference, T_A is the virtual potential temperature, and V is the flight-level wind speed) and ranged from 60%–80% over land to 70%–90% over water. Higher wind speeds reduced the bulk Richardson number to more neutral values, causing lower adjustment percentages.

Past studies (e.g., Graham and Hudson 1960) and more recent data collected in hurricanes simultaneously monitored by reconnaissance aircraft and NOAA buoys or platforms (e.g., Powell 1982; Burpee et al. 1994) indicate that surface inflow is maintained in the eyewall and within the eye and that differences between flight-level and marine surface observations are on the order of 20°. Comparisons to surface observations over land in Andrew (see Tables A2 and A3) suggest that a reasonable estimate of the surface wind direction over land may be made by subtracting 40° from aircraft measured wind directions. For this study, marine and land surface wind directions for the adjusted aircraft observations were assigned by simply subtracting 20° and 40°, respectively, from the flight-level wind directions. The resulting wind directions maintain inflow toward the circulation center within the eye. We should note that, except for eyewitness reports of calm and the onset of strong southerly winds on the back side of the eye, no surface observations were available to validate the assignment of wind directions within the eye; this will be discussed further in Powell and Houston (1996). We further note that asymmetric inflows (Powell 1982) and even outflows (Powell 1987) have been observed at the surface in landfalling hurricanes related to a background environmental flow and outer convective rainband development, respectively. No such asymmetries were apparent in the Andrew observations.

Obviously, the aircraft was too high to be considered near the PBL. Multiple flight-level research experiments and airborne Doppler radar measurements indicate that maximum mean winds in hurricanes are usually found at 0.5–2.0 km, below the 2.5–3.2-km level flown in Hurricane Andrew. However, a comparison (Powell and Black 1990) of 69 surface measurements in unstable conditions (sea surface temperature greater than buoy air temperature) to aircraft wind observations from 500-m, 1500-m, and 3000-m levels indicated no consistent difference in the ratio of surface to flight-level winds. In addition, convective updrafts and downdrafts in eyewalls of mature hurricanes tend to vertically mix peak winds above the boundary layer, which would act to decrease the difference between 700-mb winds and those at lower levels (e.g., Jorgensen 1984; Franklin et al. 1993). While the peak winds may have been higher at lower levels, a mean PBL wind would also have to include winds affected by friction at lower levels, so it is conceivable that a PBL-mean wind might be of similar magnitude to the 2.5–3.2-km-level wind. Lacking information on what the winds may have been at levels below 3 km in Andrew, we assume that the wind speeds at 2.5–3.2 km are representative of mean winds in the PBL.

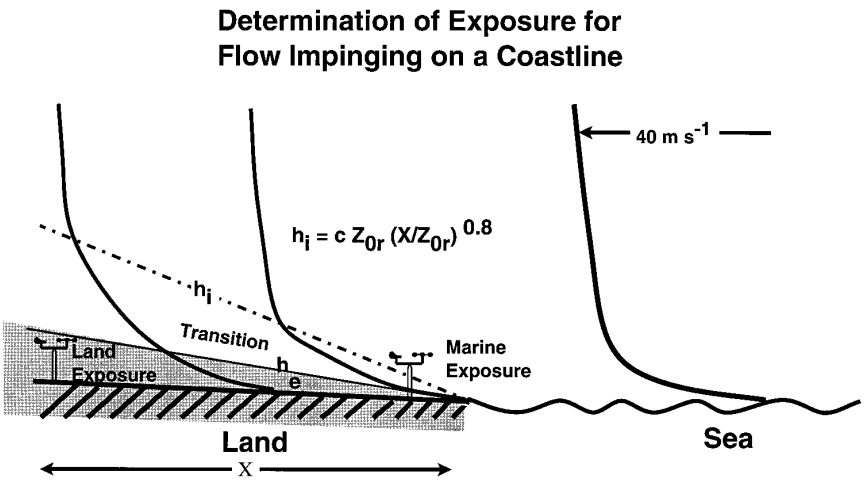

FIG. 8. Schematic of wind profile change and internal boundary layer (height h_i) development during flow from marine to land exposure. Height h_E represents the depth of the layer in equilibrium with the new underlying surface.

In order to account for a possible underestimate of the eyewall winds by the 1-min data, maximum 10-s mean flight-level wind speeds were input to the PBL model within 34 km of the center. The maximum 10-s mean winds accounted for the possibility of enhanced transfer of momentum in highly convective regions of the eyewall. Outside the core (greater than 34 km from the center) 1-min flight-level wind speeds were input to the model except for the westward inbound flight leg on the east side of the storm (as discussed above for the southeast coast landfall). Maximum 10-s mean winds were used for that entire leg.

The surface-layer formulation in the PBL model is subject to the same limitations for high-wind drag coefficients and wave effects as the Liu et al. (1979) model. Based on comparisons in a storm-relative coordinate framework (appendix A), boundary layer model adjustments of flight-level winds to maximum 1-min winds at 10 m in open exposure yield speeds within 20% of the actual surface winds with directions that are within ±20°. Failure to adjust flight-level winds to the surface will produce 20%–40% overestimates of the maximum surface wind speed and wind directions that have little inflow.

c. Adjustment to standard (open) exposure

Wind standards published in building codes (design winds) prescribe an open exposure typical of most airport weather station anemometers. Since knowledge of the surface winds that occurred during Andrew may impact future design wind criteria, we converted all input data over land to an open exposure based on photographic roughness characterizations of all major wind measurement locations. Roughness characterizations were made according to descriptive categories discussed above. All surface wind measurements over land were converted to a standard terrain roughness length of 0.03 m. By applying the relationship between friction velocity and the gradient wind (Blackadar and Tennekes 1968; Gill 1968) to two different roughness categories with the same gradient wind, Simiu and Scanlan (1986) determined

$$\frac{u_{*S}}{u_*} = \left(\frac{Z_{OS}}{Z_O}\right)^{0.0706}. \qquad (3)$$

In this case, u_{*S} is the friction velocity appropriate for the standard terrain roughness, u_* is the friction velocity appropriate for the wind measurement adjusted to 10 m as determined from the log law, Z_{OS} is the standard open-terrain roughness of 0.03 m, and Z_O is the roughness length consistent with the exposure for the given wind measurement. If the actual U_{10} for a roughness of 0.5 m was 26 m s^{-1} (u_* of 3.5 m s^{-1}), the (3)'s solution of u_{*S} is 2.85 m s^{-1}, and the open-terrain neutral stability U_{10} (computed from the log law) is 41.5 m s^{-1}. Hence, an area with open terrain would experience much greater wind speeds than an adjacent area with rougher terrain; an observation that became obvious in examining the hurricane damage. Because of uncertainties in estimation of local roughness and the influence of larger-scale upwind fetch, it was important to test roughness estimates by comparing actual open-exposure wind measurements to neighboring rough-exposure observations adjusted to open terrain. The form of (3) is relatively insensitive to Z_O estimation errors mentioned in a previous section. Applying the log law to a range of roughness lengths ±0.25 m about a ''true'' value of 0.5 m, and a 20–50 m s^{-1} range of winds, the computed 10-m-level wind can vary ±14%–23% from the true wind speed. However, after then applying (3) to convert the 10-m winds to open terrain, the speeds vary by only ±5% from the true value. Hence, after adjusting a wind measurement to 10 m and then to open terrain, the cumulative error caused by uncertainty in estimating roughness length is on the order of ±5%. Failure to adjust wind speeds to standard terrain could result in U_{10} values that are about 40% too low and prevent an analysis from resolving meaningful differences.

In general, wind measurements from marine exposures were not converted to a standard terrain but are representative of the existing sea state, subject to limitations mentioned above. However, in some cases, marine observations may be available in a location relative to the storm where no land measurements survived; such was the case in Andrew for C-MAN observations from Fowey Rocks. Consecutive 10-min mean and hourly 2-min mean winds measured at Fowey Rocks ceased at 0800 UTC when Andrew's wind center was 20 km away, approximately the same radial distance from the storm as the maximum wind measured by the air force reconnaissance aircraft at 0810 UTC. Since the Fowey Rocks observations were made in the vicinity of the eyewall in the northwest quadrant of the storm (where few observations were available over land), we converted the adjusted 10-m-level winds to what would be experienced over land in open terrain using (3) with u_* and Z_O supplied by the Liu et al. (1979) model and then applied the log law for neutral conditions.

d. Adjustment to maximum sustained wind speed

Since the maximum sustained (1-min average) wind V_{M1} is released in advisories and warnings issued to the public by NHC, all available wind data were converted to this quantity if possible. After adjustment to 10 m (and adjustment to open terrain for land exposures), observations with averaging times greater than 2 min (including adjusted aircraft observations assumed to be equivalent to 10-min mean surface winds) were adjusted to the probable maximum 1-min wind within the observation sampling period. The adjustment procedure used relationships between the 1-min gust factor

and sampling period, based on the work of Durst (1960) for level terrain flow, Krayer and Marshall (1992, hereafter KM) for hurricane winds over land, and additional hurricane data collected from NOAA buoys since 1979. This work assumes that deviations of short-period wind averages from the longer-period mean over stationary time periods of at least 1 h follow a Gaussian distribution. Unfortunately, no high-resolution wind speed data were available from Hurricane Andrew, but observations collected in Hurricane Bob (Fig. 4b) support this assumption. Krayer and Marshall define the gust factor $G_{t,\mathrm{T1}}$ as the highest t-period mean occurring over a longer averaging time period (T1):

$$G_{t,\mathrm{T1}} = 1.0 + \sigma_{t,\mathrm{T1}} * \mathrm{SND}. \quad (4)$$

In (4), $\sigma_{t,\mathrm{T1}}$ represents the standard deviation of the short t-period mean wind about the longer T_1 period mean normalized by the longer-period mean wind and SND is the standard normal deviate associated with a probability of $1 - t/\mathrm{T}_1$ available from probability tables of the normal distribution (e.g., Box et al. 1978). A $G_{60,\mathrm{T}}$ relationship was developed for several averaging periods between 120 and 3600 s. Following KM's approach, measurements of $\sigma_{t,\mathrm{T}}$ from the published sources were used with

$$\sigma^2_{t,\mathrm{T1}} = \sigma^2_{t,\mathrm{T2}} + \sigma^2_{\mathrm{T2,T1}} \quad (5)$$

to compute equivalent normalized standard deviations for time periods in which data were not available. For example, the mean gust factor $G_{5,510}$ from comparisons of NOAA buoy measurements to aircraft observations in hurricanes from 1979–85 (Powell and Black 1990) was used in (4) to solve for $\sigma_{5,510}$. This value and a Durst (1960) value of $\sigma_{5,3600}$ were used in (5) to solve for $\sigma_{510,3600}$. Finally, (5) was solved for $\sigma_{60,510}$ given $\sigma_{510,3600}$ and a published value (Durst 1960) for $\sigma_{60,3600}$. The resulting $G_{60,T}$ values (Fig. 9) were fit by a third-order polynomial valid for 120 s $< T <$ 3600 s:

$$G_{60,\mathrm{T}} = 2.6631 - 2.1244 \log_{10}\mathrm{T} + 0.85245(\log_{10}\mathrm{T})^2 - 0.10346(\log_{10}\mathrm{T})^3. \quad (6)$$

For example, this relationship increases a 10-min average wind speed by 11% ($G_{60,600} = 1.11$) to estimate the highest 1-min average that would occur over the 10-min period. Based on differences between KM and Durst's $G_{t,3600}$ curves published in KM and the standard deviation of $G_{60,600}$ from Hurricane Bob data, the accuracy of $G_{60,\mathrm{T}}$ is estimated at ± 0.03, resulting in a wind speed uncertainty of $\pm 6\%$.

Accuracy of these methods depends on the relevance of the underlying Gaussian assumption. Shortcomings include the following. 1) It is not possible to convert any 1-h averaging time of say, 1 min, to another of 10 min; we can only estimate the *highest* short-period wind that might be observed over some longer time period, or vice versa. 2) Very few datasets were available for determining $\sigma_{60,\mathrm{T}}$, and without complete wind records it is not known whether the stationarity assumption was satisfied for those data. 3) The data available to create (6) include both land (open terrain) and marine exposures; as more high-resolution digital wind velocity records become available in tropical cyclones, separate $G_{60,\mathrm{T}}$ relationships will be needed for marine and open-terrain exposures. This technique cannot be applied to typical airways hourly observations (1-min average) in the Hurricane Andrew dataset because the wind was not monitored continuously over each hour. For 5-, 10-, and 15-min average wind observations that compose the balance of the dataset, the probability of a maximum 1-min wind greater than that computed using (6) is 20%, 10%, and 7%, respectively.

5. Quality control

Many reports obtained after landfalling hurricanes require qualification due to uncertainties in position, time, exposure, or measurement. Evaluations of surface and flight-level observations were performed by nearest neighbor comparisons of plotted information in storm-relative coordinates (e.g., Fujita 1963; Miller 1964). This technique was used in reconstructing wind fields of Hurricanes Frederic, Alicia, Hugo, and Tropical Storm Marco (Powell 1982, 1987; Powell et al. 1991; Houston and Powell 1994). Since the wind field is assumed to be representative of the chosen time interval, time periods with minimal intensity changes should be chosen if possible. Plots of flight-level winds in the eye and public reports of calms and their duration in the vicinity of Homestead were used to construct a track of the circulation center. A time period of 0445–1130 UTC was chosen to depict the wind field during Andrew's landfall in south Florida; shorter time periods excluded many observations and resulted in large data-sparse areas. From 0445 to 0915 UTC central sea level pressure decreased from 93.6 to 92.2 kPa and then increased to near 94.4 kPa by 1130 UTC, while the maximum 1-min flight-level wind speeds on the north side of the storm increased from 68 m s^{-1} to a maximum of 82 m s^{-1} at 0810 UTC and then decreased to 70 m s^{-1} by 1010 UTC.

a. Treatment of peak wind observations

Several observations of the peak wind measured during the storm or the last measurement before loss of electrical power or failure of the anemometer system were brought to our attention after a public appeal for data was published in the *Miami Herald* (Wallace 1992). Frequently, there were no written or otherwise recorded values, and details of the observations were determined from interviews and site visits. Most credence was given to sites with well-exposed anemometers; several homeowner anemometers were placed too close to the roofline to provide an accurate wind

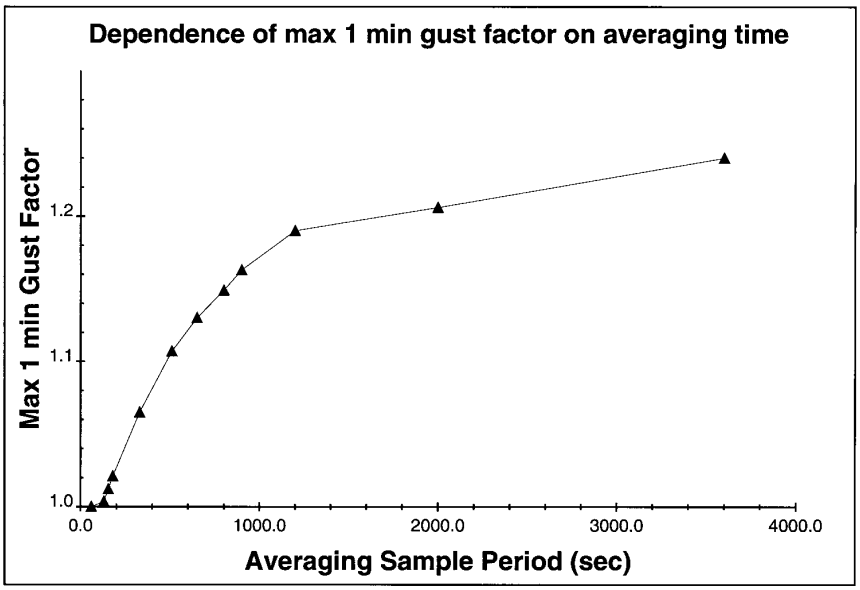

FIG. 9. Dependence of 1-min gust factor on averaging period based on data from Krayer and Marshall (1992), Durst (1960), and NOAA marine platforms in hurricanes.

measurement. Interviews or written reports obtained within 1–2 months of the storm were considered to be most accurate; followup interviews sometimes led to statements that contradicted earlier interviews. When an observation based on an interview or log was in doubt, plotting it relative to surrounding observations of known quality made it possible to accept or remove the datum.

Only one visual observation without a log was deemed sufficiently accurate to be included in the Andrew surface wind observations. This report from Perrine (PER) was a visual record of the last digital reading of the instrument (95 m s^{-1}) before the 10-m mast failed. The instrument did not survive, but we acquired three identical samples from the manufacturer for wind tunnel testing (see appendix B). Tests indicated that the instruments over estimated the true wind speed by 16.5%, suggesting that the actual gust was 79.4 m s^{-1}. A recent study by Black (1993) suggests that gust factors in landfalling hurricanes decrease with height at approximately the same rate that the mean wind in the boundary layer decreases with height, implying that peak convective downdraft gusts conserve momentum vertically. Hence, the Perrine gust was assumed to be associated with a convective downdraft in the eyewall and was not adjusted for exposure. A gust factor curve published in KM was used to convert the gust (assumed to be a 2-s mean) to a hypothetical 1-h mean (79.4/1.7 = 46.7 m s^{-1}), and the maximum 1-min wind for the hour was estimated as [(46.7)(1.32)] 61.6 m s^{-1}. This observation occurred ''sometime'' between 0830 and 0900 UTC, and no wind direction was given. Time and wind direction of the observation were estimated based on nearest-neighbor comparisons of storm-relative positions of the observation for several possible times (PER 0830, 0845, and 0900 UTC) and the location of the observation relative to the eyewall (dashed line) in Fig. 10. In this case, PER 0900 UTC was located on the inner side of the eyewall and fit in best with the 0759 UTC observation from Fowey Rocks C-MAN (marine exposure) and the peak adjusted winds from the aircraft (which are farther inward than the flight-level winds depicted in Fig. 10). It is possible that slightly higher winds may have occurred at this site following the instrument failure, but the PER 0900 UTC value is consistent with the highest surface wind estimates computed from the aircraft data.

Of special concern were reports of anemometers ''pegged'' for periods of several minutes at Tamiami Airport and at north Key Largo. Examination of archived anemometer charts from severe hurricanes (including Camille of 1969, Celia of 1970, and Frederic of 1979) confirms that eyewall winds are extremely turbulent, especially over land, with high-frequency gusts and lulls. An envelope of the lulls is typically about 40%–60% of the gust speeds. Given this ratio, a ''pegged'' value of 50 m s^{-1} at Tamiami Airport would imply peak gusts of 100–125 m s^{-1} and sustained winds of between 77 and 100 m s^{-1}. This was considered extremely unlikely since the last measurement of sustained winds at Fowey Rocks C-MAN station (with marine exposure and closer to the radius of maximum winds) was 55 m s^{-1} at 10 m. It is possible that the wind speed circuit of the F420 anemometer (which was in the process of falling off the crossarm before the tower failed, Fig. 2) picked up voltages from the di-

rection circuit causing the speed dial to read offscale (R. Marshall, National Institute of Standards and Technology, 1993, personal communication). Official reports from Tamiami Airport through 0833 UTC were considered reliable. However, the peak Tamiami Airport observation attributed to 0848 UTC was eliminated from this dataset although it is considered valid in other descriptions of Hurricane Andrew's winds (e.g., Mayfield et al. 1994).

Additional pegged anemometer reports were contained in the log of the sailboat *Mara Cu*, moored north of Key Largo (Fig. 10). According to the manufacturer, the measurement display indicated a 2–5-s mean wind, and the wind direction was given relative to the heading of the vessel. The display was limited to two digits in knots for wind speed, and the instrument was rated as accurate to ± 2 m s^{-1} up to 26 m s^{-1} (V. Valldeperis, Brooks and Gatehouse, 1995, personal communication). The deck log indicated that the reading was in excess of 51 m s^{-1} at 0833, 0840, and 0846 UTC, and the captain of the vessel estimated the winds to be much higher based on the noise. Flight-level winds adjusted to the surface in the vicinity were $\sim$50 m s^{-1}, implying gusts of $\sim$65 m s^{-1}. Given that lulls are typically 40%–60% of gusts, the *Mara Cu* winds are too strong to be considered lulls; it is likely that lulls occurred during intervals between the log entries. Given the uncertainty of what the gust and lull values may have been during these periods, and the fact that nearby surface-adjusted flight-level winds were of the same order as the log records, we assumed that the winds recorded in the *Mara Cu* log were representative of 5-min means.

b. Position of the radius of maximum winds

To properly adjust flight-level winds to the surface, it is necessary to know the location of the radius of maximum sustained winds (R_{MW}) and its variation with 1) height from the surface to the altitude of the air force reconnaissance aircraft (3 km), 2) azimuth relative to the heading of the storm, and 3) intensity as the storm weakened during landfall. Failure to account for tilt in the vicinity of the eyewall places the adjusted maximum winds from flight level too far from the surface center of the storm. Unfortunately, no continuous anemometer records were available in the core region to indicate the position of the surface R_{MW}. Studies by Hawkins and Rubsam (1968), Jorgensen (1984), and Willoughby (1988, 1990) note that above the boundary layer, in the azimuthal-mean sense, hurricane winds are in approximate gradient and thermal wind balance. The tilt (ϕ) from the horizontal of the tangential wind maximum in Hurricane Allen (1980) was shown by Jorgensen (1984) to be very close to the tilt of lines of constant angular momentum computed according to

$$\tan\phi = \left(\frac{V_\theta}{R_{\mathrm{MW}}}\right)\left(\frac{\partial V_\theta}{\partial z}\right)^{-1}, \qquad (7)$$

where V_θ is the tangential wind component, z is height, and $\partial V_\theta/\partial z$ is the vertical shear of the tangential wind. According to the thermal wind relationship given in Jorgensen (1984),

$$\partial V_\theta/\partial z = f\left[\left(\frac{2V_\theta}{R_{\mathrm{MW}}}\right) + f\right]^{-1} g(fT_{\mathrm{m}})^{-1}\left(\frac{\partial T}{\partial r}\right)_{\mathrm{p}}, \qquad (8)$$

where f is the Coriolis parameter, g is the gravitational acceleration, T_{m} is the mean temperature of the layer applying to the shear calculation, and $(\partial T/\partial r)_{\mathrm{p}}$ is the radial gradient of temperature along a constant pressure surface. According to these relationships, an intense, compact hurricane with a small R_{MW} will display very little outward slope of angular momentum surfaces. Indeed, Hawkins and Imbembo (1976) found a near-vertical R_{MW} in Hurricane Inez (1966), a very small intense hurricane very similar in size (13 km R_{MW}) and strength (67 m s^{-1} mean winds at 500 m with 10-s gusts to 81 m s^{-1}) to Andrew. This calculation (Table 2) was made for Andrew based on measurements made on the 70.0-kPa pressure surface flown by the air force aircraft. According to Table 2, R_{MW} tilt increased from 50°–60° to near 80°, while Andrew intensified from 0600 to 0900 UTC and then tended to decrease during landfall from 75° to 64°. On the south side, the R_{MW} was initially steep (due to relatively small R_{MW} and high V_{T}) at 69° and then decreased (because of an increase in R_{MW} and a decrease in V_{T}) to a more outward slope of 45° during landfall.

These measurements are unique because safety considerations have previously restricted aircraft from following a hurricane over land during landfall. The calculations suggest that the landfall process may cause the R_{MW} to tilt more outward as the winds decrease and that the effect may be asymmetric. Estimates of the R_{MW} at the surface, assuming the tilt calculated in Table 2, suggest a surface R_{MW} 1–3 km inward of that determined from the 1-min mean flight-level winds. Radially outward from the wind maxima, the time of the peak 10-s wind within each 1-min flight-level observation in the storm core was simply assigned to coincide with the inward most possible 10-s period without regard to the computed surface R_{MW} location. For example, on the south side of the storm, the time of the peak 10-s value measured by the northbound aircraft between 0801:00 and 0802:00 UTC was taken to be centered at 0801:55 UTC. The peak 1-min flight-level winds measured in Andrew occurred on a northbound leg in the northern eyewall and reached 82 m s^{-1}, with a peak 10-s mean of 83.6 m s^{-1} at 0810 UTC (the minute corresponding to 0810–0811 UTC). The peak 10-s value was attributed to 0810:05 UTC and became 60.4 m s^{-1} when adjusted to 10-m open exposure over land. Hence, PBL model-adjusted aircraft winds in the core region (vicinity of the eyewall less than 34 km

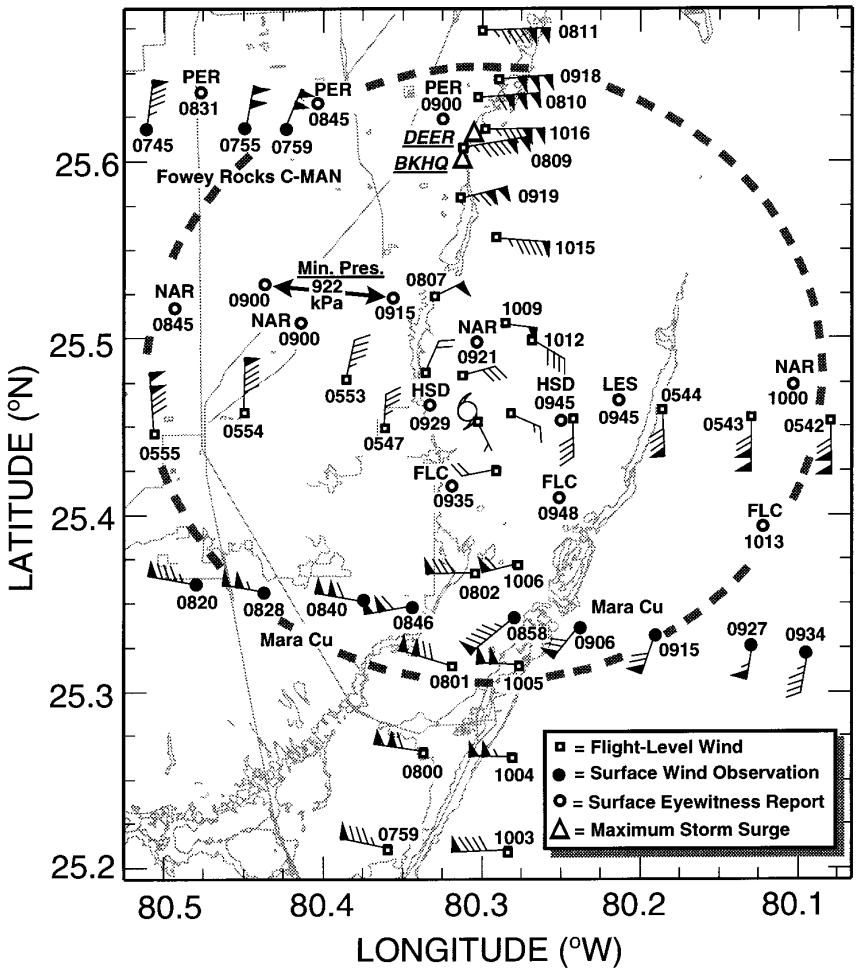

FIG. 10. Storm-relative (for 0900 UTC 24 August 1992) locations of flight-level wind speeds relative to the location of peak storm surge values measured at Burger King Headquarters (BKHQ) and the Deering Estate County Park (DEER), peak gust measured at the surface in Perrine (PER, 0900), Fowey Rocks C-MAN station (marine-exposure 10-m winds), and extreme structural damage at Naranja Lakes (NAR, 0845). Also shown are locations of calm in the eye; the minimum surface pressure measurement; the onset of strong south winds at the surface in the eyewall based on eyewitness observations at Homestead (HSD), Florida City (FLC), and Leisure City (LES); and maximum surface winds in the southern eyewall (*Mara Cu*). Dashed circle represents a trace through the peak reflectivity of the eyewall according to the Melbourne WSR-88D radar at 0902 UTC. For clarity, several aircraft and *Mara Cu* observations were omitted.

from the storm center) displayed sharper peaks that were shifted closer to the circulation center than the 1-min data alone would allow. The 10-s adjusted R_{MW} are shown in Table 2 as well as R_{MW} estimated from the thermal wind shear. In general, the assigned positions are consistent with the thermal-wind-shear-estimated positions except for the east pass and the second south pass, where the peak 10-s wind occurred inward from the time of the peak 1-min wind. Outside the core region (greater than 34 km from the storm center), 1-min PBL model-adjusted aircraft winds were not shifted in position.

Indirect measures of the surface R_{MW} were made by noting the location of peak storm surge (Fig. 10) and the time of severe damage to a townhouse relative to the locations of the maximum 1-min flight level winds. The maximum recorded storm surges (Mayfield et al. 1994) were 5.15 m above the National Geodetic Vertical Datum at Burger King Corporation (BKHQ at 15.6-km radius) and 5.06 m at the Deering Estate Park (DEER at 17.4-km radius). The surface-adjusted R_{MW} from the maximum 10-s aircraft winds (Table 2) compare very well with the positions of maximum storm surge. The time of damage to the Naranja Lakes development was documented by the time read off a stopped clock found in the building debris (P. Black, HRD, 1992, personal communication). Three of the seven deaths within structures during Andrew's south

Florida landfall were in this development despite its location in a storm surge evacuation area. The clock pinpointed the time of damage, plotted as NAR 0845 in Fig. 10. The western eyewall was over Naranja Lakes at 0845 UTC. The last observation from Fowey Rocks C-MAN station before its mast failed was coincident with the eyewall (21-km radial distance), indicating that failure occurred very close to the position of the R_{MW}.

Several observations of the eye (Fig. 10) were supplied by the public (sources are listed in the acknowledgments). Calm winds in the eye were observed in Homestead (HSD, 0929) and at Florida City (FLC, 0935). Onset of strong south winds is indicated at FLC 0948–1013, Leisure City (LES, 0945), and HSD (0945). Eyewitness reports of extreme winds on the back side of the eye based on the sound of the wind were treated cautiously. The noise level increases rapidly when new winds on the back side of the eye become strong enough to carry debris. Small debris that had been deposited from the front side of the storm suddenly becomes airborne, and the density of the debris field (and its attendant noise) is greater than on the front side of the eyewall, leading to the perception of much stronger winds. Unfortunately, no surface measurements are available to document wind conditions in the Homestead area during that time. The minimum pressure in the eye (Mayfield et al. 1994) was measured northwest of the circulation center, from 0900 to 0915 UTC about midway between the circulation center and the eyewall. Calm winds were not observed at the location of the pressure minimum. A separation of pressure, wind, and radar centers is probably quite common in hurricanes but difficult to document due to lack of data. Relative to the direction of motion, Andrew's wind center was displaced to the left of the radar center and to the left and behind the pressure center. When compared relative to the positions of maximum winds in the southern eyewall from the sailing vessel *Mara Cu* and the positions of the maximum flight-level aircraft winds on the east and south sides, it appears that the R_{MW} was only 10–15 km on the south and east sides of the storm, perhaps in response to the displacement of the pressure center.

c. Final wind observation distribution

After completion of the standardization steps and quality control described above, the distribution of land-exposure observation locations over the ~7-h time period chosen to apply to southeast Florida is displayed in Fig. 11 with geography corresponding to the time of landfall (0900 UTC). Note the change in data density from the west to the east side of the storm center associated with anemometer system failures. A separate distribution (not shown) contains the marine-exposed observations over the same time period. These data at each site conform to the same framework for height, exposure, and averaging time and are now suitable for input to an objective analysis scheme. Analysis of these data and observations from Andrew's exit from Florida's west coast are discussed in the companion paper (Powell and Houston 1996).

6. Conclusions

A review of spectral analyses conducted in past hurricanes suggest that the turbulent, convective, and perhaps mesogamma scales contribute most to the energy of the wind fluctuations. Surface-layer similarity theory scaling is applicable to horizontally homogeneous motion characterized by mechanical and buoyancy-produced turbulence in quasi-stationary conditions. Similarity methods advocated here do not take into account possible scaling factors associated with curved flow, upstream roughness changes, clouds, and mesoscale phenomena but appear reasonable for height adjustment of ~10-min mean winds in the surface layer. Maximum 1-min winds were computed from longer-period averages (or in the case of Perrine from a single peak gust value) by using gust factor relationships that assume a Gaussian distribution of normalized deviations of short-period means about longer-period means. This assumption is supported by high-resolution surface data collected during Hurricane Bob (1991).

TABLE 2. Calculations of the tilt of the R_{MW} in the eyewall of Hurricane Andrew. Here, V_T is peak (1-min average flight-level wind speed); dV_Z thermal wind shear; Tilt slope of the eyewall wind maximum from horizontal; 1 min R_{MW} (R_{MW} based on maximum 1 min flight-level winds); $S_{FC}R_{MW}$ R_{MW} at the surface computed from tilt; and 10-sR_{MW} R_{MW} based on estimated position of peak 10-s wind at flight level.

Eyewall location	Time of pass (UTC)	1 min R_{MW} (km)	V_T (m s^{-1})	dV_Z (m s^{-1} km^{-1})	Tilt (deg)	$S_{FC}R_{MW}$ (km)	10-sR_{MW} (km)
North	0806–0813	19.6	82.0	−0.95	77.2	18.9	18.7
	0915–0920	20.9	76.8	−1.08	73.6	20.0	17.8
	1012–1019	18.0	70.1	−1.51	68.9	16.8	15.1
South	0757–0803	15.9	61.4	−1.27	71.8	15.0	13.6
	0921–0926	22.2	50.5	−2.29	44.8	19.2	11.6
	1002–1010	21.9	53.1	−2.24	47.2	19.1	19.5
East, west	0544–0553	23.0	62.9	−2.00	53.7	20.8	15.9
	0553–0558	19.8	66.4	−1.74	62.7	18.2	17.8

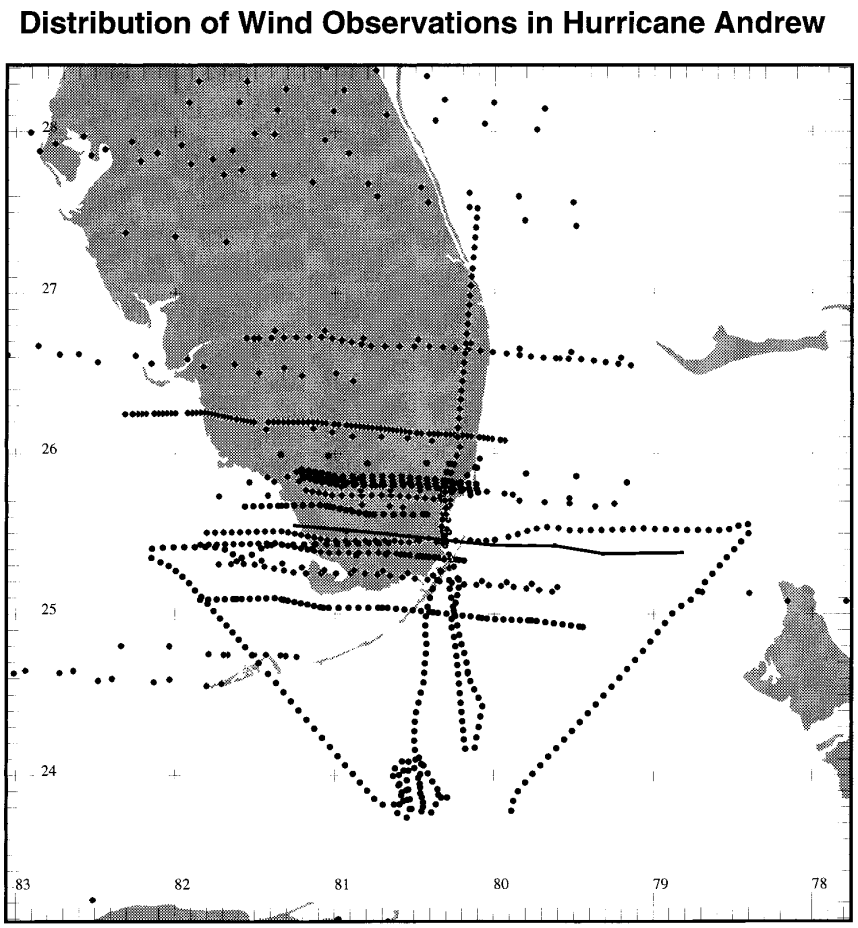

FIG. 11. Final distribution of wind data locations for Andrew's landfall in southeast Florida. Geography is positioned relative to Andrew's circulation center at 0900 UTC 24 August 1992. Crosshairs are plotted at 1° latitude–longitude intervals. Solid line represents the storm track.

In order for a wind field analysis to be useful to forecasters or the public, all input data should conform to a common standard framework. This framework is defined by the warning and advisory requirements of NHC, guidelines for surface wind measurement, and by wind loading provisions of building codes. Here, we defined the framework as the maximum 1-min sustained wind speed at the 10-m level over open terrain (for land analyses) or over an observed or modeled sea state (for oceanic analyses). Hence, all input data must undergo screening and adjustment procedures to conform as closely as possible to the framework. A measure of the error of each standardizing procedure and the consequences of not following each procedure is shown in Table 3. For a 50 m s^{-1} wind speed, assuming the errors in Table 3 are representative of standard deviations, the total error was computed by summing the variance contributions of the height-exposure and time procedures. For oceanic observations the error is on the order of 7% while it is 10.5% for land observations.

For the present, the procedures applied to the Hurricane Andrew observations appear to resolve many of the wind speed discrepancies caused by differences in terminology, exposure, measurement height, averaging period, and terrain and are simple enough to be used in analyzing a historical or real-time wind field. These procedures are only valid for relatively uniform terrain typical of many coastal areas. They are not applicable to locations characterized as mountainous or complex terrain. In such areas, a marine-exposure analysis should be conducted, and the resulting field then used as an initial condition to a mesoscale model capable of resolving flow over complex terrain or to a wind tunnel model of the effected area. The companion paper (Powell and Houston 1996) examines objective streamline and isotach analyses of the surface wind field and potential products for real-time disaster response, recovery, and damage mitigation activities.

Anemometer system failures in landfalling hurricanes will continue to occur until survivable design,

TABLE 3. Estimated accuracy and consequence error of wind standardization procedures.

Procedure	Procedure error	Consequence error
Marine platforms		
Adjustment to 10 m	±3%	15%–30%
Adjustment to max 1 min		
All averaging times over 2 min	±6%	15%–25%
Land platforms		
Adjustment to 10 m	±7%	15%–30%
Adjustment to standard exposure	±5%	30%–40%
Adjustment to max 1 min		
All averaging times over 2 min	±6%	15%–25%
Reconnaissance aircraft		
PBL model adjustment to 10 m, standard exposure, max 1 min (based on comparisons with nearby surface observations)	±20%	20%–40%

installation, and exposure guidelines are followed. Many of these guidelines are now contained in a standard for surface wind measurement devised at a 1992 workshop organized by the Federal Coordinator for Meteorology at the request of the Interdepartmental Hurricane Conference (OFCM 1992). This standard is currently undergoing submission to the American Society for Testing and Materials. With eventual adoption universally, a wide variety of wind equipment manufacturers and users will have access to the information needed for a successful installation and archival. If the proposed standard is adopted in the United States, ASOS will require changes to comply with these standards in order to improve the chances that future anemometers will survive hurricanes (Powell 1993).

Acknowledgments. This research was supported in part by the Coastal Hazards element of NOAA's Coastal Ocean Program and Florida Power and Light Corporation (FPL) Grant 93MGD03. Bret Christoe and Neal Dorst of HRD helped to perform site surveys and reduce data. Joyce Berkeley of HRD and Shirley Murillo of MAST Academy also helped with data reduction. Much useful data were acquired with assistance from NHC including former director Dr. Bob Sheets, Deputy Director Jerry Jarrell, Dr. Ed Rappaport, and John Parr, and from the Miami NWS Forecast Office staff under the leadership of Paul Hebert. Special thanks go to the public of south Florida, who responded to our request for data, especially Randy Fairbank, John Bigelow, Peter Skipp, Debbie Iacovelli, Allan DeParle, Mrs. G. Hall, Mr. B. Martens. Thanks also to Dan Adams of FPL, Janet Bravo of Metro Dade County Water and Sewer Department, Eric Swartz of the South Florida Water Management District, Tom Ross of the National Climatic Data Center, Steve Gill of the National Ocean Service, Bob Panko and DeWitt Smith of Everglades National Park, Amy Kazmier of Big Cypress National Preserve, David Holmes of the Dade County Agricultural Extension Service, David Crane of the Florida Division of Forestry, Eric Meindl, Dave Gilhousen, and Mike Burdette of the NOAA National Data Buoy Center, George Priest, David Fleming, Don Groot, and Michael Greco of the FAA, and Billy Wagner of Monroe County Civil Defense. Gale Carter and Eric Dutton of the 53rd Air Force Reserves Weather Squadron (Hurricane Hunters) and John Pavone of CARCAH assisted with acquisition and interpretation of the air force reconnaissance observations. Mike

TABLE A1. Characteristics of selected surface observation sites. Record types: *d* = digital, *T* = trace, *I* = interview, and *L* = log. Gust notes: *C* = from center runway anemometer (FA1), *PT* = peak within averaging time (Tavg.), and *PH* = peak during hour. *Za* = anemometer height, *Zo* = roughness length, *D* = zero-plane displacement, and Marine = Liu model results converted to open terrain exposure with 0.03-m roughness.

Station ID	*Za* (m)	Record type	Tavg (min)	Freq Samples h^{-1}	Gust notes	*Zo* (m)	*D* (m)	Source
FA2	12.2	*d*	1	60	*C*	.30–.50	2.–3.	FAA/LLWAS
FA4	12.4	*d*	1	60	*C*	.20–1.00	1.–6.	FAA/LLWAS
FP1	10	*T*	10	6	*PT*	0.075	0	FP&L Turkey Point
FSW	60, 10	*T*	10	6	*PT*(From 60-m level)	0.075	0	FP&L 6 mi. SW of Turkey Point
HAU	13.7	*d*	2	1	*PH*	Marine	Marine	NOAA/NOS
JOE	10.1	*d*	15	4	*PT*	.01–.03	0	National Park Service
MaraCu	16.7	*L*	5	2	*PT*	.08–.30	3	J. Bigelow
MBY	3.5	*d*	15	2	*PT*	.01–.10	0–1.0	National Park Service
MLR	14.7	*d*	10	6	*PH*	Marine	Marine	NOAA/NDBC
NHC	46	*T*	10	6	*PT*	.20–1.00	3.–6.	NOAA/NHC
PER	10	*I*	3 sec	1	Final digital readout of instrument	—	—	R. Fairbank
VKY	13.7	*d*	1	1	*PH*	0.2	1	Metro Dade Water and Sewer

Black, Paul Leighton, Bret Christoe, Peter Dodge, and Chris Samsury recorded and analyzed the WSR-57 radar measurements in Hurricanes Andrew and Bob. Chuck Long of the U.S. Army Engineer CERC Field Research Facility provided wind data collected in Hurricane Bob. James Acquistapace of Davis Instruments provided the anemometers for wind tunnel testing, and the Civil Engineering Department of the Virginia Polytechnic Institute and State University provided the wind tunnel. Much useful critical input was provided by reviews of earlier versions of this manuscript by anonymous reviewers and by Dr. Robert Sheets and the hurricane specialists of NHC, Dr. Robert Burpee, Dr. Peter Black, John Kaplan, Peter Dodge, and Paul Willis of HRD, Dr. Wilson Shaffer of the NWS Techniques Development Lab, Dr. Richard Marshall of the National Institute of Standards and Technology, Dr. John Peterka of the Colorado State University Civil Engineering Department, former NHC director Dr. Robert Simpson, and Jeff Keppert of the Australian Bureau of Meteorology Research Center. Mention of a manufacturer or product does not constitute an endorsement of the U.S. Department of Commerce, NOAA, or the authors.

APPENDIX A

Comparisons of Surface and Aircraft Observations

The accuracy of adjusting flight-level measurements to the surface was estimated by comparison to surface platforms in a storm-relative framework satisfying stringent time and spatial separation criteria. Characteristics of the surface observation platforms used in the comparisons are shown in Table A1. Both land-based and model-adjusted aircraft winds represent maximum 1-min sustained winds for open exposure at 10 m as discussed above; gusts are raw values that have undergone no adjustments. Only nine independent comparisons were possible in the core region (radial distance less than 34 km) with time differences less than 1.1 h, distance separations of less than 10 km, and radial and azimuthal distance separations of 5 and 10 km. Comparisons in Table A2 suggest that the sustained surface winds were 72% of the flight-level peak 10-s wind speeds, with values ranging from 57% to 103%. Model-adjusted winds tended to be greater than the closest surface observations (bias of 5%) and the root-mean-square (rms) difference was 21% (± 9 m s^{-1}). Surface-adjusted aircraft wind directions showed an rms difference of $\pm 16°$, and surface wind gusts were 64%–103% (mean 83%) of the nearest flight-level maximum 10-s value. Much of the variability in the comparisons may be due to changes occurring over relatively small time and space differences between the positions of the aircraft and surface observations. This variability is not surprising given the extreme radial gradient in wind speed, and the azimuthal or temporal variation in convective activity at a given radius. Also important is the comparison of the highest

TABLE A2. Comparisons of the closest surface observations (S_{FCOB}) to maximum 10-s flight-level and surface-adjusted aircraft winds within 34 km of Andrew's wind center. Here, WS_{SFC}, WD_{SFC} is observed surface wind speed and direction; WS_{ACSFC}, WD_{ACSFC} surface wind speed from PBL model and assigned direction for aircraft data; WS_{AC}, WD_{AC} flight-level wind speed and direction; $WS_{SFC/AC}$ ratio of observed surface wind speed to flight-level wind speed; Gust/WS_{AC} ratio of observed surface gust to flight-level wind speed; Time diff S_{FC}. observation time–Aircraft time; DelS Distance separation between sfc. observation and aircraft; and NA data not available.

S_{FCOB}	Time (UTC)	WS_{SFC} (m s^{-1})	WD_{SFC} (deg)	Gust (m s^{-1})	Radius (km)	A/C time (UTC)	WS_{ACSFC} (m s^{-1})	WD_{ACSFC} (deg)	WS_{AC} (m s^{-1})	WD_{AC} (deg)	$WS_{SFC/AC}$	Gust/WS_{AC}	Time diff (hhmmss)	DelS (km)
Mara Cu	0846:00	57.4	260	NA	13.8	0802:05	43.8	228	59.4	268	0.97	NA	4355	5.8
Mara Cu	0901:00	48.8	231	NA	13.8	1006:05	35.5	216	47.3	256	1.03	NA	−10505	1.3
Mara Cu	0909:00	35.3	220	48.9	16.0	0922:55	30.2	213	47.3	256	0.75	1.03	1355	5.6
Mara Cu	0915:00	35.2	200	46.4	18.3	0923:05	45.7	230	62.2	270	0.57	0.75	805	2.6
MBY	0938:00	32.4	211	NA	29.1	0924:05	41.3	221	55.9	261	0.58	NA	1355	8.4
NHC	0900:00	43.1	45	>51.5*	28.1	0812:05	49.1	48	67.4	88	0.64	0.68	4755	2.7
NHC	0910:00	44.1	45	>51.5*	27.4	0917:55	55.0	51	75.9	91	0.58	0.64	755	2.9
PER	0900:00	60.9	45	79.4	18.5	0809:55	57.9	41	79.9	81	0.76	0.99	5005	2.6
VKY	0830:00	34.4	58	50.6	32.9	0813:05	41.3	50	56.0	91	0.61	0.90	1655	0.4
										Means	0.72	0.83		

* NHC's trace went off scale.

TABLE A3. Comparisons of the closest surface observations to maximum 1-min flight-level and surface-adjusted aircraft winds greater than 34 km from Andrew's wind center.

S_{FCOB}	Time (UTC)	WS_{SFC} (m s^{-1})	WD_{SFC} (deg)	Gust (m s^{-1})	Radius (km)	A/C time (UTC)	WS_{ACSFC} (m s^{-1})	WD_{ACSFC} (deg)	WS_{AC} (m s^{-1})	WD_{AC} (deg)	$WS_{SFC/AC}$	Gust/WS_{AC}	Time diff (hhmmss)	DelS (km)
FA2	0855:00	27.2	56	34.5	41.4	1020:30	33.9	52	48.8	92	0.56	0.71	−12530	2.0
FA2	0905:00	26.1	64	35.6	40.9	0814:30	34.6	55	49.8	95	0.52	0.71	05030	1.8
FA2	0915:00	26.9	69	32.5	41.2	0915:30	38.0	57	54.8	97	0.49	0.59	00030	1.4
FA4	0855:00	33.3	57	34.5	35.5	1019:30	36.3	47	52.4	87	0.64	0.66	−12430	0.6
FA4	0905:00	32.2	64	35.6	35.1	0916:30	41.4	53	59.6	93	0.54	0.60	01130	1.5
FP1	0725:00	20.7	315	22	56.4	0601:30	22.0	338	31.8	17	0.76	0.69	12330	1.8
FP1	0735:00	22.9	310	26	50.2	0600:30	24.9	336	35.9	16	0.74	0.73	13430	2.2
FP1	0745:00	25.7	310	29.1	44.0	0559:30	27.1	333	39.0	14	0.72	0.75	14530	2.3
FP1	0755:00	31.2	305	32.7	37.8	0558:30	30.9	330	44.5	10	0.66	0.73	15630	2.2
FSW	0525:00	12.2	330	17.9	117.3	0610:30	16.0	347	23.1	27	0.53	0.77	04530	3.8
FSW	0545:00	11.1	332	17	106.9	0609:30	16.1	353	23.4	33	0.47	0.73	02430	2.5
FSW	0555:00	11.9	335	18.4	102.7	0608:30	17.3	350	25.0	30	0.47	0.74	01330	0.4
FSW	0615:00	14.7	330	25.6	94.6	0607:30	19.1	348	27.7	28	0.53	0.92	00730	1.9
FSW	0625:00	15.5	325	22.9	90.6	0606:30	19.2	350	27.7	30	0.56	0.83	01830	3.4
FSW	0705:00	17.8	315	25.6	73.6	0604:30	19.5	348	28.2	27	0.63	0.91	10030	6.3
FSW	0715:00	18.6	312	25.1	67.4	0603:30	20.0	347	29.0	27	0.64	0.87	11130	6.3
FSW	0725:00	19.4	315	26.9	61.3	0602:30	21.3	344	30.7	24	0.63	0.88	12230	6.4
HAU	0900:00	24.0	90	43.7	53.6	0913:30	30.3	63	43.7	103	0.55	1.00	01330	0.7
JOE	0523:00	10.2	317	11.3	135.6	0613:30	13.2	344	19.2	24	0.53	0.59	05030	6.9
JOE	0553:00	11.6	311	13.3	120.9	0611:30	15.9	345	22.9	25	0.51	0.58	01830	7.1
JOE	0938:00	33.3	220	37.9	28.9	1003:30	31.6	228	45.6	268	0.73	0.83	02530	2.4
JOE	1023:00	28.8	196	32.4	36.8	0925:30	28.4	214	40.9	254	0.70	0.79	05730	2.8
Mara Cu	0615:00	14.4	320	NA	83.8	0605:30	19.2	346	27.6	26	0.52	NA	00930	3.8
MBY	0508:00	11.8	310	10.2	131.9	0612:30	14.8	346	21.3	26	0.55	0.48	−10430	4.0
MBY	0908:00	31.8	234	22.9	25.8	0759:30	30.7	242	44.2	282	0.72	0.52	10830	4.4
MLR	0855:00	20.6	253	29.1	50.9	0755:30	15.7	237	22.7	277	0.91	1.28	05930	2.9
MLR	0905:00	21.0	249	NA	50.4	0756:30	18.8	243	27.1	283	0.77	NA	10830	7.1
MLR	0915:00	20.8	243	NA	50.8	0959:30	18.5	207	26.7	247	0.78	NA	04430	5.3
MLR	0925:00	20.8	236	30.3	55.0	0929:30	16.4	206	23.8	246	0.88	1.27	00430	3.9
NHC	0900:00	43.1	45	⩾51.5	28.1	1018:30	41.3	45	59.6	85	0.72	NA	−11830	2.4
VKY	0830:00	34.4	58	50.6	32.9	0813:30	37.4	51	54.0	91	0.64	0.94	01630	2.6
									Means		0.63	0.78		

model-adjusted aircraft wind (which was slightly outside the separation criteria) with the highest surface measurement. The highest winds measured at the surface (PER) were within 0.5 m s^{-1} of the highest adjusted aircraft wind on the north side of the storm and 5% of the nearest adjusted aircraft surface wind. The highest surface gust at PER was nearly identical to the closest flight-level 10-s gust.

Outside the eyewall vicinity (radial distance greater than 34 km), with the space separation criteria as above and time differences of less than 2 h, 31 comparisons in Table A3 suggest that maximum 1-min surface winds for open terrain were 63% of the flight-level 1-min wind speeds with ratios ranging from 47% to 90%. Model-adjusted aircraft winds overestimated surface observations by 14% (2.4 m s^{-1}), with an rms difference of 19% ($\pm$3.7 m s^{-1}). Surface-adjusted aircraft wind directions showed an rms difference of $\pm$20°, and surface wind gusts were 50%–100% (mean of 78%) of the nearest flight-level 1-min value except near the Molasses Reef C-MAN station, where gusts were nearly 30% higher than the 1-min flight-level wind speeds.

APPENDIX B

Evaluation of Digitar Weather-Master Anemometers

Surface data from Hurricane Andrew in south Florida included a single peak reading from a Davis Instruments Digitar Weather-Master anemometer on a 10-m mast in the Perrine area. The peak reading was 95 m s^{-1} or 212 mph as actually read from the digital readout and was widely reported in the news media. A site visit indicated that the anemometer was well exposed and warranted further evaluation to assess its accuracy. The 95 m s^{-1} speed was well beyond the instrument's specified operating range.

Three anemometer samples were obtained from the manufacturer and tested in the Stability Wind Tunnel at Virginia Polytechnic Institute and State University (VPISU). The stability tunnel is a low-turbulence, aeronautical closed-circuit facility. Its test section is 2 m by 2 m, which allowed testing of the anemometers with minimal blockage. The top speed approaches 90 m s^{-1} with no obstruction in the wind tunnel. Wind velocities are uniform within less than 1% throughout the middle of the test section, and speeds are measured

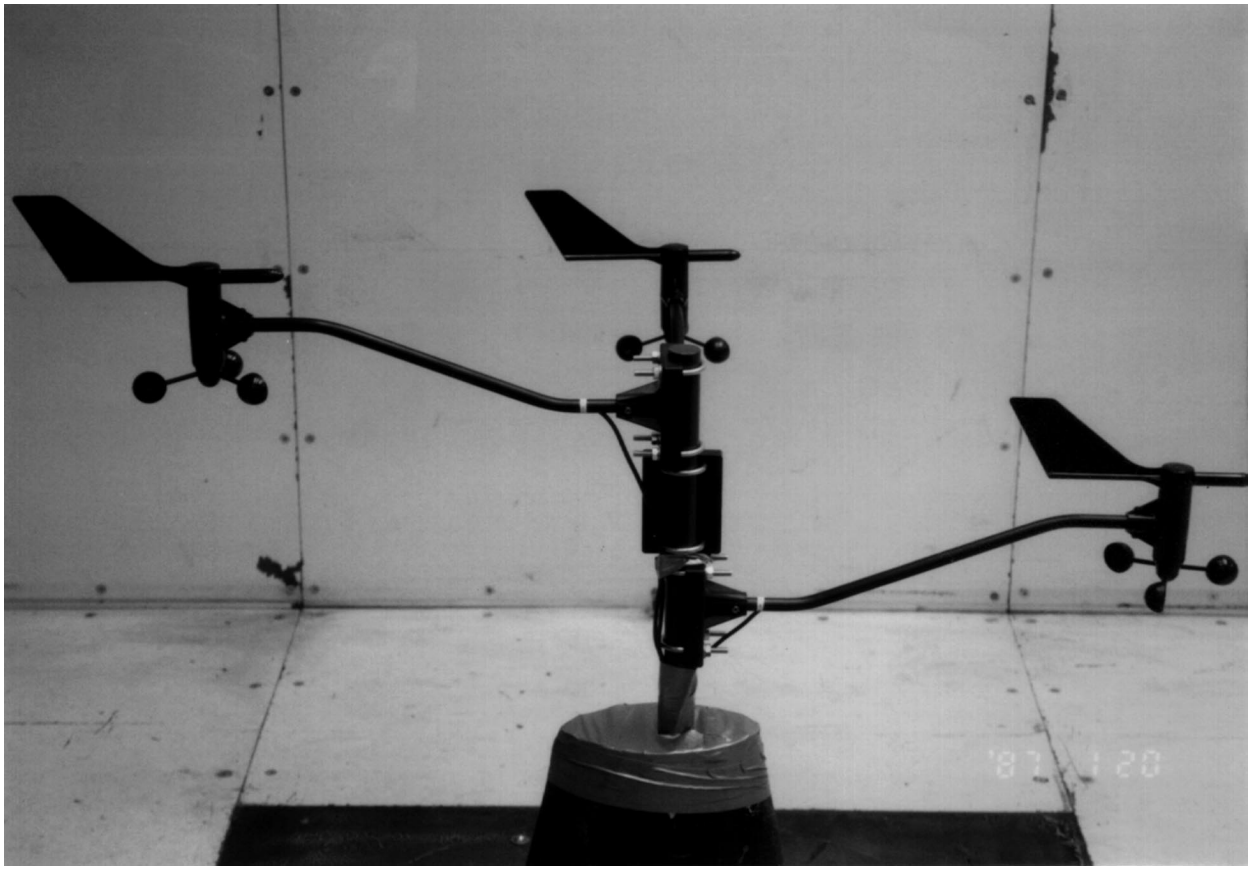

FIG. B1. Initial configuration of three sample anemometers in the Virginia Polytechnic Institute and State University wind tunnel. Tunnel section (and wind flow) runs right to left. Dimension from left to right ~1 m.

using a certified electronic Barocell Micro-manometer connected to a standard pitot tube. Speeds measured in the wind tunnel at velocities greater than about 9.0 m s^{-1} are accurate within less than 1%.

Prior to testing, the instruments were mounted in a lower-speed wind tunnel at Clemson University and operated for several hours to allow the anemometers to seat themselves. At VPISU the anemometers were initially mounted as shown in Fig. B1 with one anemometer oriented upstream, one downstream, and one to the side of the support mast. Two sets of tests were conducted, one with the anemometers in this orientation and one with the anemometers oriented upstream or to the side of the support. Test procedures involved increasing the wind tunnel speed in increments of about 2.25 m s^{-1} starting at 9.0 m s^{-1}. Once the wind tunnel speed had been set, digital readings from the anemometers were recorded, and the wind speed was increased to the next increment. In the first test sequence, wind tunnel speeds were varied between 9.0 and 54 m s^{-1}. The anemometers were then repositioned such that anemometer 1 was pointed into the wind, upstream of the support and that anemometers 2 and 3 were oriented to the left and right sides of the support, respectively. In this configuration, each of the anemometers were exposed to flow that was undisturbed by the other anemometers.

The second set of tests involved increasing the wind tunnel speed to a speed where one or more of the anemometers failed. Anemometers 1 and 3 (Fig. B2) provided almost identical output, while anemometer 2 provided somewhat lower velocities. Both anemometers 1 and 3 failed at a wind speed of 78 m s^{-1}. The mode of failure was the fracture of the plastic arm holding the plastic cup at the hub. It is likely that the centrifugal forces from the spinning cups exceeded the tensile capacity of the connection at the hub. Since the anemometers use the rotation of a magnet in the cup assembly to produce a pulse that is counted by the meter, the results indicate that anemometers 1 and 3 were spinning at the same rotational velocity when they failed and that anemometer 2 was spinning at a slightly lower rate, probably due to slightly higher friction (anemometer 2 consistently spun at lower rates during the first tests as well).

The anemometers provide reasonably accurate readings up to about 40 m s^{-1}. Above 40 m s^{-1}, the measured velocities tend to exceed actual steady wind speeds, and the deviation increases with wind speed. The facilities available did not provide for the determination of length constants for the Digitar anemometers or the assessment of possible over- or undershoot when the anemometers are subjected to gusty winds. Conversations with Davis Instruments staff suggested that anemometers in the field would generally spin more easily than new units, and they suggested the break-in period. Based on these conversations and consistency of anemometer performance, first-order corrections to the Perrine field data were based on the results from anemometers 1 and 3. Thus, a 16.5% reduction was applied to the field data resulting in a peak gust of 79.4 m s^{-1}.

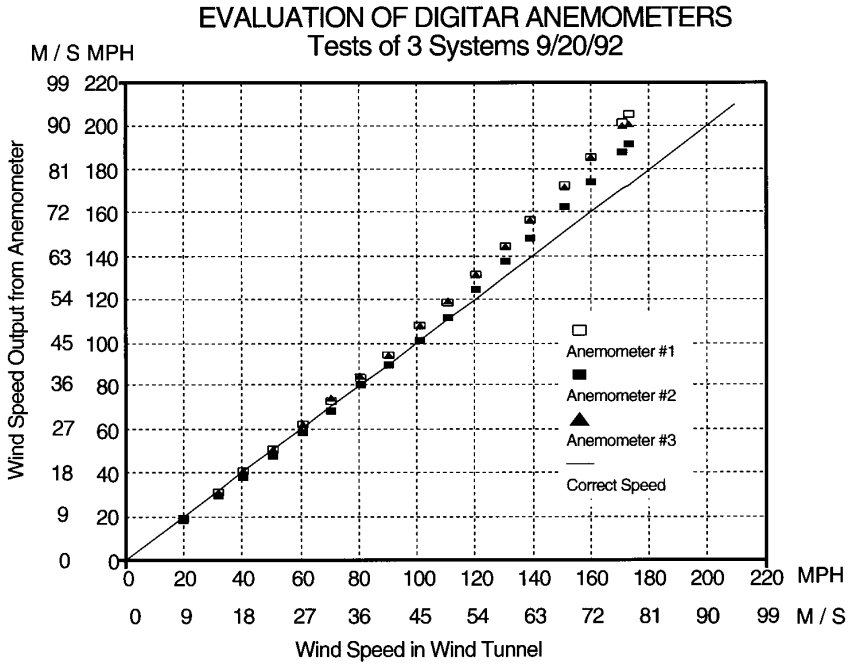

FIG. B2. Wind tunnel calibration results of three anemometers shown in Fig. B1. Wind speed units are shown in meters per second and miles per hour.

REFERENCES

Arya, S. P., 1988: *Introduction to Micrometeorology.* Academic Press, 307 pp.

ASCE, 1994: Minimum design loads for buildings and other structures. ASCE Note 7-93, American Society of Civil Engineers, 134 pp.

Black, P. G., 1993: Evolution of maximum wind estimates in typhoons. *Proc. ICSU/WMO Int. Sym. on Tropical Cyclone Disasters,* Beijing, China, Int. Council of Scientific Unions, 104–115.

——, and S. H. Houston, 1994: Comparison of NOAA and Air Force wind measurements in Hurricane Emily near Cape Hatteras. *Minutes of the 48th Interdepartmental Hurricane Conf.,* Miami, FL, Federal Coordinator for Meteorological Services and Supporting Research, A33–A41. [Available from Office of the Federal Coordinator for Meteorological Services and Supporting Research, Suite 1500, 8455 Colesville Rd., Silver Spring, MD 20910.]

Blackadar, A. K., and H. Tennekes, 1969: Asymptotic similarity in the planetary boundary layer. *J. Atmos. Sci.,* **26,** 1015–1020.

Box, G. E. P., W. G. Hunter, and J. S. Hunter, 1978: *Statistics for Experimenters.* Wiley and Sons, 653 pp.

Burpee, R. W., and Coauthors, 1994: Real-time guidance provided by NOAA's Hurricane Research Division to forecasters during Emily of 1993. *Bull. Amer. Meteor. Soc.,* **75,** 1765–1783.

Charnock, H., 1955: Wind stress on a water surface. *Quart. J. Roy. Meteor. Soc.,* **81,** 639–640.

Cline, I. M., 1926: *Tropical Cyclones.* The MacMillan Co., 301 pp.

Davenport, A. G., 1961: The spectrum of horizontal gustiness near the ground in high winds. *Quart. J. Roy. Meteor. Soc.,* **87,** 192–211.

Deardorff, J. W., 1972: Parameterization of the planetary boundary layer for use in general circulation models. *Mon. Wea. Rev.,* **100,** 93–106.

Durst, C. S., 1960: Wind speeds over short periods of time. *Meteor. Mag.,* **89,** 181–186.

Forristall, G. Z., 1988: Wind spectra and gust factors over water. *Proc. Offshore Technology Conf.,* Houston, TX, OTC, 449–460. [Available from University of Miami RSMAS Library, 4600 Rickenbacker Cswy., Miami, FL 33149-1098.]

Franklin, J. L., S. J. Lord, S. E. Feuer, and F. D. Marks Jr., 1993: The kinematic structure of Hurricane Gloria (1985) determined from nested analyses of dropwindsonde and Doppler radar data. *Mon. Wea. Rev.,* **121,** 2433–2451.

Fujita, T. T., 1963: Analytical mesometeorology: A review. *Severe Local Storms, Meteor. Monogr.,* No. 27, Amer. Meteor. Soc., 77–125.

Garratt, J. R., 1977: Review of drag coefficients over oceans and continents. *Mon. Wea. Rev.,* **105,** 915–929.

Gill, A. E., 1968: Similarity theory and geostrophic adjustment. *Quart. J. Roy. Meteor. Soc.,* **94,** 586–588.

Graham, H. E., and G. Hudson, 1960: Surface winds near the center of hurricanes (and other cyclones). NHRP Rep. 39, 200 pp. [Available from NOAA/AOML Library, 4301 Rickenbacker Cswy., Miami, FL 33149.]

Hawkins, H. F., and D. T. Rubsam, 1968: Hurricane Hilda, 1964. II. Structure and budgets of the hurricane on October 1, 1964. *Mon. Wea. Rev.,* **96,** 617–636.

——, and S. M. Imbembo, 1976: The structure of a small, intense hurricane—Inez 1966. *Mon. Wea. Rev.,* **104,** 418–442.

Houston, S. H., and M. D. Powell, 1994: Surface winds and water level response during Tropical Storm Marco (1990). *Wea. Forecasting,* **9,** 427–439.

Janjic, Z. I., 1994: The step-mountain eta coordinate model: Further developments of the convection, viscous sublayer, and turbulence closure schemes. *Mon. Wea. Rev.,* **122,** 927–945.

Janssen, P. A. E. M., 1989: Wave-induced stress and the drag of air flow over sea waves. *J. Phys. Oceanogr.,* **19,** 745–754.

Jorgensen, D. P., 1984: Mesoscale and convective-scale characteristics of mature hurricanes. Part II: Inner core structure of Hurricane Allen (1980). *J. Atmos. Sci.,* **41,** 1287–1311.

Katsaros, K. B., S. D. Smith, and W. A. Oost, 1987: HEXOS: Humidity Exchange Over the Sea, a program for research on water vapor and droplet fluxes from sea to air at moderate to high wind speeds. *Bull. Amer. Meteor. Soc.,* **68,** 466–476.

Krayer, W. R., and R. D. Marshall, 1992: Gust factors applied to hurricane winds. *Bull. Amer. Meteor. Soc.,* **73,** 613–617.

Landsea, C. W., 1993: A climatology of intense (or major) Atlantic hurricanes. *Mon. Wea. Rev.,* **121,** 1703–1713.

Large, W. G., and S. Pond, 1981: Open ocean momentum flux measurements in moderate to strong winds. *J. Phys. Oceanogr.,* **11,** 324–336.

Larsen, S. E., K. Hedegaard, and I. Troen, 1982: The change of terrain roughness problem extended to mesoscale fetches. *Proc. First Int. Conf. on Meteorology and Air/Sea Interaction,* The Hague, the Netherlands, Amer. Meteor. Soc. and Roy. Netherlands Meteor. Inst., 8–13.

Liu, W. T., K. B. Katsaros, and J. A. Businger, 1979: Bulk parameterizations of air–sea exchanges of heat and water vapor including the molecular constraints at the interface. *J. Atmos. Sci.,* **36,** 1722–1735.

Mayfield, M., L. A. Avila, and E. N. Rappaport, 1994: The Atlantic hurricane season of 1992. *Mon. Wea. Rev.,* **122,** 517–538.

Miller, B. I., 1964: A study on the filling of Hurricane Donna (1960) over land. *Mon. Wea. Rev.,* **92,** 389–406.

NHC, 1992: Hurricane Andrew Preliminary Report. 36 pp. [Available from National Hurricane Center, 11691 SW 117th St., Miami, FL 33165-2149.]

OFCM, 1992: *Minutes of the 46th Interdepartmental Hurricane Conference.* 229 pp. [Available from Office of the Federal Coordinator for Meteorological Services and Supporting Research, Suite 1500, 8455 Colesville Rd., Silver Spring, MD 20910.]

——, 1993a: *Minutes of the 47th Interdepartmental Hurricane Conference.* 406 pp. [Available from Office of the Federal Coordinator for Meteorological Services and Supporting Research, 8455 Colesville Rd., Suite 1500, Silver Spring, MD 20910.]

——, 1993b: National hurricane operations plan. 125 pp. [Available from Office of the Federal Coordinator for Meteorological Services and Supporting Research, Suite 1500, 8455 Colesville Rd., Silver Spring, MD 20910.]

Panofsky, H. A., and J. A. Dutton, 1984: *Atmospheric Turbulence.* Wiley Interscience, 397 pp.

Peterson, E. W., 1969: Modification of mean flow and turbulent energy by a change in surface roughness under conditions of neutral stability. *Quart. J. Roy. Meteor. Soc.,* **95,** 561–575.

Powell, M. D., 1980: Evaluations of diagnostic marine boundary layer models applied to hurricanes. *Mon. Wea. Rev.,* **108,** 757–766.

——, 1982: The transition of the Hurricane Frederic boundary layer wind field from the open Gulf of Mexico to landfall. *Mon. Wea. Rev.,* **110,** 1912–1932.

——, 1987: Changes in the low-level wind kinematic and thermodynamic structure of Hurricane Alicia (1983) at landfall. *Mon. Wea. Rev.,* **115,** 75–99.

——, 1993: Wind measurement and archival under the Automated Surface Observing System (ASOS): User concerns and opportunity for improvement. *Bull. Amer. Meteor. Soc.,* **74,** 615–623.

——, and P. G. Black, 1990: The relationship of hurricane reconnaissance flight-level measurements to winds measured by NOAA's oceanic platforms. *J. Wind Eng. Ind. Aerodyn.,* **36,** 381–392.

——, and S. H. Houston, 1996: Hurricane Andrew's wind field at landfall in south Florida. Part II: Applications to real-time analysis and preliminary damage assessment. *Wea. Forecasting,* **11,** 329–349.

——, P. P. Dodge, and M. L. Black, 1991: The landfall of Hurricane Hugo in the Carolinas: Surface wind distribution. *Wea. Forecasting,* **6,** 379–399.

Sempreviva, A. M., S. E. Larsen, N. G. Mortensen, and I. Troen, 1990: Response of neutral boundary layers to changes of roughness. *Bound.-Layer Meteor.,* **50,** 205–225.

Simiu, E., and R. H. Scanlan, 1986: *Wind Effects on Structures.* Wiley Interscience, 589 pp.

Simpson, R. H., and H. Riehl, 1981: *The Hurricane and Its Impact.* Louisiana State University Press, 398 pp.

Singer, I. A., C. M. Nagle, and R. M. Brown, 1961: Variation of wind with height during the approach and passage of Hurricane Donna. NHRP Rep. 50, 408 pp. [Available from NOAA/AOML Library, 4301 Rickenbacker Cswy., Miami, FL 33149.]

Tuttle, J. D., and B. Gall, 1995: Radar analysis of Hurricanes Andrew and Hugo. Preprints, *21st Conf. on Hurricanes and Tropical Meteorology,* Miami, FL, Amer. Meteor. Soc., 608–610.

van der Hoven, I., 1957: Power spectrum of horizontal wind speed in the frequency range of 0.0007 to 900 cycles per hour. *J. Meteor.,* **14,** 160–164.

Wallace, R., 1992: How fast was Andrew? Engineers, meteorologists disagree. *Miami Herald,* September 6, p. 24a. [Available from Miami Herald Publishing Co., One Herald Plaza, Miami FL 33132-1693.]

WERC, 1992: Hurricane Andrew—Preliminary observations of the WERC post disaster team. 5 pp. [Available from Wind Engineering Research Council, Inc., P.O. Box 10029, College Station, TX 77842.]

Wieringa, J., 1992: Updating the Davenport roughness classification. *J. Wind Eng. Ind. Aerodyn.,* **41,** 357–368.

Willoughby, H. E., 1988: The dynamics of the tropical cyclone core. *Aust. Meteor. Mag.,* **36,** 183–191.

——, 1990: Gradient balance in tropical cyclones. *J. Atmos. Sci.,* **47,** 265–274.

Wood, D. H., 1982: Internal boundary layer growth following a step change in surface roughness. *Bound.-Layer Meteor.,* **22,** 241–244.